THE JOURNAL OF BIOLOGICAL CHEMISTRY
Vol. 271, No. 35, Issue of August 30, pp. 21583–21596, 1996
Printed in U.S.A.

Purification and Structural Characterization of a Filamentous, Mucin-like Proteophosphoglycan Secreted by *Leishmania* Parasites*

(Received for publication, April 17, 1996, and in revised form, June 20, 1996)

Thomas Ilg‡§¶, York-Dieter Stierhof‖, David Craik, Richard Simpson‡‡, Emanuela Handman‡, and Anthony Bacic§**

*From the ‡Walter and Eliza Hall Institute of Medical Research, P. O. Royal Melbourne Hospital, Victoria 3050, Australia, the ‖Max-Planck-Institut für Biologie, D-72076 Tübingen, Federal Republic of Germany, **Centre for Drug Design and Development, University of Queensland, Brisbane, Queensland 4072, Australia, ‡‡Ludwig Institute for Cancer Research and the Walter and Eliza Hall Institute of Medical Research, Joint Protein Structure Laboratory, Victoria 3050, Australia, and the §Plant Cell Biology Research Centre, School of Botany, University of Melbourne, Victoria 3052, Australia*

Parasitic protozoa of the genus *Leishmania* secrete a filamentous macromolecule that forms networks and appears to be associated with cell aggregation. We report here the purification of this parasite antigen from *Leishmania major* culture supernatant and its compositional (75.6% carbohydrate, 20% phosphate, 4.4% amino acids, w/w), structural, and ultrastructural characterization as a highly unusual proteophosphoglycan (PPG). Mild acid hydrolysis, which cleaves preferentially hexose 1-phosphate bonds, releases the PPG glycans. Their structures are Galβ1–4Man, Manα1–2Man, Galβ1–3Galβ1–4Man, PO_4-6(Galβ1–3)$_{0-2}$Galβ1–4Man, and PO_4-6(Araβ1–2Galβ1–3)Galβ1–4Man. These glycans are also components of the parasite glycolipid lipophosphoglycan, but their relative abundance and structural organization in PPG are different. Some of them represent novel forms of protein glycosylation. ^{31}P NMR on native PPG demonstrates that phosphate is exclusively in phosphodiester bonds and that the basic structure R-Manα1-PO_4-6-Gal-R connects the glycans. A phosphodiester linkage to phosphoserine (most likely R-Manα1-PO_4-Ser) anchors the PPG oligosaccharides to the polypeptide. PPG has a unique amino acid composition; glycosylated phosphoserine (>43 mol %), serine, alanine, and proline account for more than 87 mol % and appear to be clustered in large proteinase-resistant domains. Electron microscopy of purified PPG reveals cable-like, flexible, long (to 6 μm), and unbranched filaments. The overall structure of PPG shows many similarities to mammalian mucins. Potential functions of this novel mucin-like molecule for the parasites are discussed.

Parasitic protozoa of the genus *Leishmania* are the causative agent of a wide range of human and animal diseases, which are transmitted by an insect vector, the sandfly. The digenetic life cycle of the parasite encompasses the infective metacyclic and several forms of procyclic, extracellular promastigotes in the digestive tract of the insect and the intracellular amastigotes residing in parasitophorous vacuoles of the mammalian host cells, the macrophages. Expression of complex and unique glycoconjugates appears to be crucial for the survival and development of the parasites in the sandfly vector and the mammalian host (reviewed in Refs. 1–3). The dominant cell surface glycolipid of *Leishmania* promastigotes is lipophosphoglycan (LPG).[1] In the sandfly, LPG serves as a ligand for the attachment of procyclic promastigotes to the midgut wall lining and may protect the parasites against the hydrolytic environment of the insect's digestive tract. After transmission of metacyclic promastigotes to the mammalian host, LPG confers complement resistance; it has been shown to act as a receptor for invasion of macrophages and may protect the parasites against the microbicidal response of the host cell (reviewed in Refs. 1, 2).

The structure of LPG from five different *Leishmania* species has been described (4–10), including life stage- and strain-specific features (8, 11, 12). Conserved structural elements are a lyso-alkylphosphatidylinositol membrane anchor, a phosphohexasaccharide core structure, and a backbone of up to 40 phosphodiester-linked disaccharides of the structure PO_4-6-Galβ1–4Man. Species-, strain-, and stage-specific modifications include glucose-1-PO_4 linked to the core structures of some LPGs, carbohydrate side chains on the phosphodisaccharide repeats, and the structures of the terminating neutral (cap) glycans.

More recently it has been reported that acid phosphatases secreted by promastigotes of various *Leishmania* species are modified by LPG-related glycans (13–16). Secreted acid phosphatase (sAP) from *Leishmania mexicana* is a highly glycosylated and phosphorylated enzyme, organized as an unusual filamentous polymer (17). Structural analysis of the *L. mexicana* sAP glycans revealed the modification of Ser(P) by unsubstituted and glucosylated phosphodisaccharides and/or mannooligosaccharides, representing a novel type of protein glycosylation (18). Specific serine/threonine-rich sequence motifs clustered near the C terminus of the sAP polypeptides appear to be the sites for this phosphoglycan modification (19).

Ultrastructural studies on the release of polymeric sAP and other macromolecular compounds from the flagellar pocket of *L. mexicana* led to the identification of a second, distinct, type

* This work was supported by the Australian National Health and Medical Research Council and by a fellowship from the Deutsche Forschungsgemeinschaft to (T. I.). The costs of publication of this article were defrayed in part by the payment of page charges. This article must therefore be hereby marked "*advertisement*" in accordance with 18 U.S.C. Section 1734 solely to indicate this fact.

¶ To whom correspondence should be addressed. Fax: 0061-3-93470852; E-mail: Ilg@wehi.edu.au.

[1] The abbreviations used are: LPG, lipophosphoglycan; PPG, proteophosphoglycan; sAP, secreted acid phosphatase; mAb, monoclonal antibody; PAGE, polyacrylamide gel electrophoresis; HPLC, high performance liquid chromatography; GC-MS, gas chromatography-mass spectrometry; ELISA, enzyme-linked immunosorbent assay; GdmCl, guanidinium chloride; BSA, bovine serum albumin; Ser(P), phosphoserine; TOCSY, total correlation spectroscopy; DQFCOSY, double quantum filtered correlation spectroscopy; HMBC, heteronuclear multiple bond correlation; T_2, spin lattice relaxation time; PG, phosphoglycan; HF, hydrofluoric acid.

of phosphoglycan-modified filamentous secretory product. This material forms fibrous networks in the center of promastigote aggregates and in the culture medium (20). Based on metabolic labeling and immunoprecipitation studies, a novel phosphate-containing secreted *Leishmania* antigen with very low electrophoretic mobility in SDS-polyacrylamide gels has been proposed as the candidate molecule. The secretion of network-forming filamentous phosphoglycan antigens by promastigotes appears to be ubiquitous in the genus *Leishmania* (3, 20), implying an important function for these macromolecular structures.

In the present study, we describe the purification of this novel filamentous phosphoglycan-modified secretory compound from *Leishmania major* promastigotes. Structural and ultrastructural studies characterize this antigen as a proteophosphoglycan (PPG) with organization and properties similar to the mammalian mucins.

EXPERIMENTAL PROCEDURES

Parasites—Promastigotes of *L. major* LRC-L137, clone V121, were grown *in vitro* in semi-defined medium 79 (21) supplemented with 5% heat-inactivated fetal calf serum (Flow).

Purification of PPG—Two liters of spent culture medium of late log/early stationary phase promastigotes (1–1.5 × 10^8 cells/ml) were passed at a flow rate of 120 ml/h over a DE52-cellulose column (12 × 3 cm; Whatman) equilibrated with 100 mM NaCl, 20 mM Tris-HCl, pH 7.5. After washing with equilibration buffer (200 ml), bound PPG was eluted with a linear gradient of 100–500 mM NaCl in 20 mM Tris-HCl, pH 7.5 (150 ml), at a flow rate of 60 ml/h. PPG-containing fractions were collected, adjusted to 1 M $(NH_4)_2SO_4$, and applied onto an octyl-Sepharose column (15 × 1.5 cm; Pharmacia Biotech Inc.) equilibrated with 1 M $(NH_4)_2SO_4$, 5 mM Na_2EDTA, 20 mM Tris-HCl, pH 7.5. The column was consecutively washed with equilibration buffer, 20 mM Tris-HCl, pH 7.5, and 50% 1-propanol (40 ml, respectively). PPG-containing flow-through fractions were subjected to ultracentrifugation (3 h, 144,000 × *g*, Ti 60 rotor, Beckman). The pellet was resuspended in 3.56 M CsCl, 5 mM Na_2EDTA, pH 7.5 (ρ = 1.45 g/ml) and ultracentrifuged for 3 h at 215,000 × *g*. The PPG pellet was resuspended in H_2O, again subjected to ultracentrifugation (3 h, 144,000 × *g*) to remove residual salt, and then dissolved in H_2O.

Alternatively, the concentrated octyl-Sepharose eluate (Centricon 30, Amicon) was applied onto a Superose 6 gel filtration column (30 × 1 cm, Pharmacia) equilibrated with 250 mM ammonium acetate, pH 7, at a flow rate of 0.5 ml/min. Both PPG- and PG-containing fractions were collected and concentrated by Centricon 30 ultrafiltration. PPG was identified throughout the purification procedure by phosphate determination, two-site ELISA, and SDS-PAGE (see below). Culture supernatant and DE52-cellulose flow-through were treated with proteinase K (100 μg/ml, 3 h, 55 °C, Boehringer Mannheim) to degrade the serum proteins present in these samples before loading onto an SDS-polyacrylamide gel. The electrophoretic mobility of PPG was not affected by this treatment (see below).

Analytical Procedures—Protein and phosphate were determined as described previously (22, 23). In the case of *L. major* culture supernatant, free phosphate and phosphate-containing low molecular weight compounds were removed by extensive ultrafiltration (Centricon 3, Amicon) prior to analysis. The values obtained were corrected for the phosphate content of identically treated fresh culture medium. Quantification of purified PPG was based on a PO_4 content of 20% (w/w). Two-site ELISA of *L. major* PPG was performed as described previously for *L. mexicana* sAP (18) using mAb AP3 (IgM) as capture antibody and biotinylated mAbs AP3, WIC79.3, or WIC108.3 or LT6 hybridoma supernatant as detecting antibodies (see Refs. 16, 24 for antigen specificities). Discontinuous SDS-PAGE (25) was performed on 4% stacking gels of either 0.2- or 1.5–2-cm length over 7.5–20% separating gels. For Western blots (26) and dot blots (1-μl aliquots of column fractions) either nitrocellulose membranes (0.2 μm, Schleicher & Schuell) or cationized nylon membranes (Zeta probe, Bio-Rad) were used. Stains-all (Bio-Rad) staining of phosphoglycan antigens in SDS-polyacrylamide gels and their immunodetection on membrane supports has been previously described (16). Silver staining of Stains-all-stained polyacrylamide gels was performed as described in Ref. 27. PPG was also analyzed on agarose gels (0.6% agarose in 40 mM Tris acetate, 4 mM Na_2EDTA, pH 7.8; 5 V/cm, 2–3 h) after the addition of 0.2 volume of sample buffer (0.25% bromphenol blue, 0.25% xylencyanol, 15% Ficoll). *Hin*dIII-cut λ-phage DNA (Promega) was used as molecular weight marker and the gels were stained with Stains-all.

Extensive biotinylation of PPG (1 mg in 750 μl of 50 mM $NaHCO_3$, pH 9.6, 37 °C) was performed by adding 3 × 25 μl of 75 mM NHS-LC-Biotin (Bio-Rad) dissolved in dimethyl sulfoxide at 2-h intervals. Biotinylated PPG was recovered by ultracentrifugation as described above.

PPG was reduced by incubation in 6 M guanidinium chloride (GdmCl), 250 mM Tris-HCl, pH 8.5, 5 mM Na_2EDTA containing 20 mM dithiothreitol for 2 h at 50 °C. Alkylation was either performed by the addition of a 5-fold molar excess of iodoacetamide over dithiothreitol and incubation in the dark for 1 h at room temperature or by adding 0.2 volume of vinylpyridine and incubation for 45 min at room temperature. The reaction was quenched by 0.2 volume of 2-mercaptoethanol. Reduced and alkylated PPG was concentrated by ultrafiltration (Centricon 30, Amicon) and applied onto a Superose 6 column equilibrated with 6 M GdmCl, 50 mM Tris-HCl, pH 8.0, 5 mM Na_2EDTA.

Enzyme Treatment of Native PPG—PPG (~50 μg) in 20 μl of 100 mM Tris-HCl, pH 8.0, 2 mM $CaCl_2$ was incubated with either trypsin (10 μg, Sigma), proteinase K (10 μg) at 37 °C or with thermolysin (10 μg, Boehringer Mannheim) at 55 °C for 1 h. The proteinases were inactivated by heating to 100 °C for 10 min, and the samples were analyzed by SDS-PAGE and agarose gel electrophoresis. To obtain larger amounts of thermolysin-cleaved antigen, PPG (500 μg) was dissolved in 100 mM Tris-HCl, pH 8.0, 2 mM $CaCl_2$ containing proteinase (20 μg) and incubated for 5 h at 55 °C. The samples were adjusted to 6 M GdmCl, 5 mM Na_2EDTA and subjected to Superose 6 chromatography in the same buffer.

Deglycosylation of PPG—PPG was subjected to mild acid hydrolysis (20 mM HCl, 15 min, 100 °C (5, 6, 28)), neutralized with 250 mM ammonium acetate, lyophilized, and dissolved in H_2O. The acid-released neutral and phosphorylated oligosaccharides were separated by high pH anion exchange HPLC on a Dionex BioLC Carbohydrate analyzer (Dionex Corp., Sunnyvale, Ca) using a Carbo-Pac PA1 column and pulsed amperometric detection using three sequential linear gradients of sodium acetate (0 mM for 6 min, raised to 50 mM over 18 min, to 175 mM over 1 min, and to 250 mM over 30 min). Peak fractions were neutralized immediately with 2 M acetic acid, desalted by passage over AG50X12 (H^+) (Bio-Rad), and lyophilized. In some experiments the protein backbone of PPG was separated from the released glycans by repeated ultrafiltration (Centricon 3, Amicon) of the hydrolysate. The filtrate and the retentate were lyophilized and subjected to monosaccharide analysis.

Enzyme Treatment of Glycans—Phosphoglycans were dephosphorylated by incubation with calf intestine alkaline phosphatase (400 units/ml, Sigma) in 50 mM NH_4HCO_3, pH 8.5, for 16 h at 37 °C. Neutral glycans were treated with jack bean α-mannosidase (10 units/ml, Sigma) or bovine testes β-galactosidase (0.2 units/ml, Boehringer Mannheim) in 50 mM sodium acetate pH 5.0, for 16 h at 37 °C. Subsequently, the samples were desalted by passage over a tandem column of AG3X4 (OH^-) (Bio-Rad) over AG50X12 (H^+), lyophilized, and rechromatographed by HPLC on a Carbo Pac PA1 column.

Gas Chromatography-Mass Spectrometry (GC-MS)—Combined GC-MS was performed using a Finnigan MAT1020B GC-MS (Finnigan, Sunnyvale, Ca), fitted with either a 25-m × 0.3-mm CPSil5 low polarity column (Chrompack, Middleburg, The Netherlands) for trimethylsilyl derivatives and permethylated alditol acetates (PMAAs) or a 25-m × 0.22-mm BPX-70 high polarity column (SGE, Australia) for alditol acetates and PMAAs as described previously (12, 29).

Monosaccharide and Methylation Analysis—Native PPG (20 μg) containing *scyllo*-inositol as an internal standard and monosaccharide standards were subjected to methanolysis, re-*N*-acetylated, and following trimethylsilylation analyzed by GC-MS either directly or after methylation with diazomethane (30) as described previously (9, 12). Alternatively, neutral monosaccharides of native, mild acid-treated, and HF-dephosphorylated PPG (20 μg, respectively) were also analyzed as alditol acetates, prepared and analyzed by standard methods (31). Methylation linkage analysis of dephosphorylated glycans (0.5–20 μg) was performed as described previously (7, 12, 18).

NMR Spectroscopy—All NMR spectra were recorded on a Bruker ARX 500 spectrometer at a temperature of 300 K. One-dimensional ^1H NMR spectra were recorded at 500.13 MHz with a spectral width of 5050 Hz, a pulse length of 7.5 μs (60°), accumulation of typically 16 scans (up to 512 scans), and with a relaxation delay between scans of 3 s. Spectra were processed using an exponential line broadening function of 0.3 Hz. Some spectra were processed using a Gaussian window function for resolution enhancement to assist in the measuring of coupling constants. Chemical shifts were referenced to 2,2-dimethyl-2-silapentane-5-sulfonate at 0.0 ppm. One-dimensional ^{31}P NMR spectra

were recorded at 202 MHz with a spectral width of 5000 Hz, a pulse width of 5 μs (45°), and a relaxation delay between scans of 2 s. Typically 500 scans were acquired prior to Fourier transformation. Spectra were processed using an exponential line broadening function of 5–10 Hz. Chemical shifts were referenced to an external capillary of 85% H_3PO_4 at 0.0 ppm. A pH titration was carried out by recording ^{31}P spectra over the pH range 3.4–9.2. Two-dimensional-DQFCOSY and TOCSY (80-ms mixing time) spectra were recorded over a spectral width of 3030 Hz in both dimensions, with 4096 data points in *F2* and 256 experiments in *F1*, each of 64 scans. HMBC spectra were recorded using 2048 complex data points in *F2* over a spectral width of 2000 Hz centered at the frequency of the residual HOD signal. This signal was suppressed by mild presaturation (75 db) during the relaxation delay. A total of 32 scans was recorded for each 128 slices over a spectral width of 800 Hz in *F1*. A relaxation delay of 1 s was used between scans, with an evolution delay of 50 ms in the HMBC sequence. While this is not tuned precisely to the expected size of the CH_2-O-P coupling, a series of trial experiments showed that it resulted in optimum signal to noise, presumably due to a compromise between the optimum evolution time for coupling (1/2*J*) and the loss of signal due to relaxation for longer delays. The two-dimensional data were processed as a 2048 × 1024 matrix, with a squared sine bell window function applied in both dimensions.

HF Dephosphorylation—PPG (50–1000 μg) was lyophilized, cooled, and mixed with pre-cooled (−20 °C) 40% aqueous HF (50–200 μl, BDH Chemicals, Australia). After 48–60 h at 0 °C, the samples were frozen in liquid N_2 and lyophilized over NaOH, redissolved in 50 mM NH_4HCO_3, and lyophilized again. HF-treated PPG was dissolved in 6 M GdmCl, 50 mM Tris-HCl, pH 8.5, 5 mM Na_2EDTA and applied at 0.5 ml/min to a Superose 6 column equilibrated in the same buffer. Fractions were analyzed for optical density at 280 nm, phosphate and by immunodot blot. Bovine serum albumin and phosvitin were used as controls for detection of peptide bond cleavage and complete protein dephosphorylation, respectively. In some experiments the protein backbone of PPG was separated from the released glycans by repeated ultrafiltration (Centricon 3, Amicon) of the hydrolysate as described above.

Amino Acid Analysis—Amino acid determinations were performed after hydrolysis of PPG (20–100 μg) with 6 M HCl, 0.1% phenol (500 μl) at 110 °C for 16–20 h *in vacuo*. After evaporation of the HCl, free amino acids were analyzed on a Beckman amino acid analyzer (model 6300).

Phosphoamino Acid Analysis—To detect phosphorylated amino acids, PPG (100 μg) was subjected to partial acid hydrolysis (6 M HCl, 0.1% phenol, 100 μl, 90 min at 110 °C). Dried hydrolysates were converted to phenylthiocarbamyl derivatives and analyzed by reversed-phase HPLC (Picotag, Waters) as described previously (32) except for using 300 mM sodium acetate at pH 5.5 instead of pH 6.5. Phosvitin, phosphoserine (Ser(P)), phosphothreonine, and phosphotyrosine and an amino acid standard mixture (Sigma) were used as controls. Norleucine (Sigma) was added as an internal standard to all samples. In some analyses, PPG, phosvitin, and Ser(P) were subjected to various treatments prior to hydrolysis. The samples were incubated at 22 and 100 °C in 20 mM ammonium acetate or at 100 °C in 20 mM HCl for 15 min. Subsequently, the samples were adjusted to 100 mM NH_4HCO_3, pH 8.5, and incubated at 37 °C for 16 h with and without the addition of calf intestine alkaline phosphatase (100 units/ml). After lyophilization, the samples were subjected to phosphoamino acid analysis as described above.

Production of Antisera—Rabbits were immunized subcutaneously with antigen resuspended in phosphate-buffered saline, emulsified in 50% complete Freund's adjuvant for the first immunization, and in 50% incomplete Freund's adjuvant in all subsequent booster immunizations. Synthetic polyserine (Sigma), or the insoluble peptide pellet of 0.5 mg of mild acid-treated *L. major* PPG, or 0.33 mg of HF-dephosphorylated PPG repurified by Superose 6 chromatography in the presence of 6 M GdmCl were used as antigens for immunization. Serum was obtained 10–14 days after each booster immunization yielding anti-polyserine (anti-PS), anti-mild acid-insoluble peptide (anti-MIP), and anti-HF-peptide (anti-HFP) antibodies. The presence of specific antibodies was assessed by dot blot and Western blot using the respective antigens and native PPG.

Electron Microscopy—Purified PPG was dissolved in 40% glycerol (50 μg/ml) and sprayed onto freshly cleaved mica. Mica pieces were transferred to a Balzers BAF 300 evaporation unit, rotary-shadowed with platinum/carbon at an angle of 8°, and backed with carbon. Replicas were floated onto H_2O and mounted on 400-mesh grids (33). PPG was also absorbed to pioloform and carbon-coated grids and negatively stained with Nano-W (Nanoprobes, Brookhaven, NY). For negative staining immunoelectron microscopy, adsorbed PPG was incubated with the mAbs LT6, WIC79.3, AP3, and LT8.2 (16) and stained with 1% aqueous uranyl acetate as described previously (20). In the case of LT6 labeling, the signal was enhanced by a subsequent incubation with ProteinA-6 nm gold.

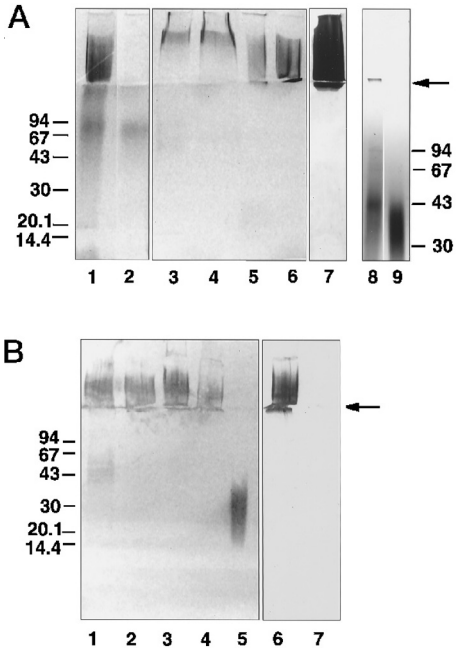

FIG. 1. **Analysis of *L. major* PPG purification by SDS-PAGE and SDS-PAGE immunoblot.** *A*, SDS-PAGE: *lane 1, L. major* promastigote culture supernatant (40 μl); *lane 2*, DE52-cellulose flow-through (40 μl); *lane 3*, DE52-cellulose eluate; *lane 4*, octyl-Sepharose eluate; *lane 5*, Superose 6 eluate (peak A); *lane 6*, pellet after ultracentrifugation in CsCl; the loading of *lanes 3–6* was normalized to a PO_4 content of 750 ng; *lane 7*, purified PPG (25 μg); *lane 8*, *L. major* PG (Superose 6 eluate, peak B) (2 μg); *lane 9, L. major* LPG (2 μg). *Lanes 1–6* and *8, 9* were stained with Stains-all, *lane 7* was stained with Stains-all followed by silver staining. *B*, SDS-PAGE immunoblot: *lane 1*, DE52-cellulose eluate; *lane 2*, octyl-Sepharose eluate; *lane 3*, Superose 6 eluate (peak A); *lane 4*, pellet after ultracentrifugation in CsCl; the loading of *lanes 1–4* was normalized to a PO_4 content of 375 ng; *lane 5, L. major* LPG (1 μg); *lane 6*, biotinylated PPG (4 μg); *lane 7*, PPG (4 μg). *Lanes 1–5* were probed with the mAb WIC108.3; *lanes 6* and *7* were probed with alkaline phosphatase-labeled avidin. The boundary of stacking and separating gel is marked by an *arrow*. The positions of standard proteins and their molecular mass in kDa is indicated.

RESULTS

Purification of PPG—It has been previously shown that the candidate antigen for the fibrous phosphoglycan-modified networks formed among *L. major* promastigotes, identified in the current study as a proteophosphoglycan (PPG), remains at the top of the separating gel in discontinuous SDS-PAGE (3, 20). In this study, the 4% acrylamide stacking gel was enlarged (from 0.2 to ~1.5–2 cm). This modification resulted in almost complete retention of PPG in this part of the SDS-polyacrylamide gel and allowed assessment of impurities migrating in the separating gel (Fig. 1).

PPG present in *L. major* promastigote culture supernatant could be detected by SDS-PAGE followed by staining with Stains-all. When the spent culture medium was subjected to anion exchange chromatography on DE52-cellulose, PPG bound quantitatively to the column (Fig. 1*A*, *lanes 1–3*). A large proportion of the LPG and phosphoglycan (PG) also present in promastigote culture supernatant (3, 34, 35) did not bind. Elution of the bound material by a NaCl gradient and analysis of the eluate by phosphate determination and by two-site ELISA yielded broad, overlapping peaks (not shown) containing PPG, LPG/PG, and various proteins, as judged by SDS-PAGE/Stains-

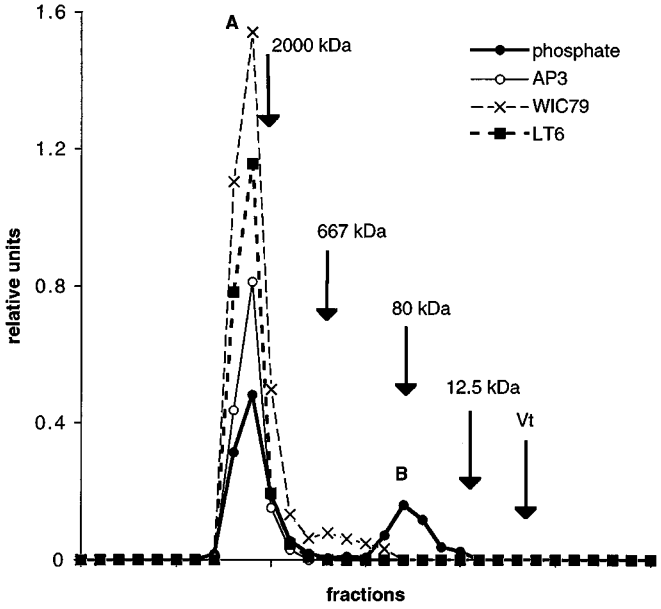

FIG. 2. **Gel filtration chromatography of *L. major* PPG.** The PPG-containing octyl-Sepharose eluate was chromatographed on Superose 6 in 250 mM ammonium acetate. Fractions were monitored for phosphate and for reactivity to the mAbs AP3, WIC79.3, and LT6 in a two-site ELISA. The elution position of dextran blue (2000 kDa), thyroglobulin (667 kDa), transferrin (80 kDa), cytochrome *c* (12.5 kDa), and the inclusion volume (V_t, CTP) of the column are indicated.

all staining (Fig. 1*A*, *lane 3*) and silver staining (not shown). The pooled DE52-cellulose fractions were then passed over octyl-Sepharose under high salt conditions and eluted stepwise with a high salt buffer, a low salt buffer, and 50% 1-propanol. The majority of PPG (>90%) and PG were recovered in the high salt wash (Fig. 1*A, lane 4*), whereas most proteins and LPG remained bound. Ultracentrifugation of the PPG-containing octyl-Sepharose flow-through led to the quantitative recovery of the antigen in a glassy, voluminous pellet, as judged by SDS-PAGE (not shown). PPG was purified further by resuspending the pellet in a CsCl solution. The high density of the solvent (ρ = 1.45 g/ml) ensured flotation of most proteins and glycoproteins (36) in a second ultracentrifugation, whereas PPG was quantitatively recovered in the pellet. PPG was desalted by resuspension in H_2O followed by ultracentrifugation and analyzed by SDS-PAGE (Fig. 1*A, lane 6*).

In an alternative purification procedure, octyl-Sepharose flow-through containing small amounts of PPG (<200 μg) were concentrated and applied onto a Superose 6 gel filtration column. Two phosphate-containing peaks were observed (Fig. 2, *peaks A* and *B*). *Peak A* eluted in the void volume, earlier than the 2000-kDa marker, and overlapped with the two-site ELISA signal obtained with three anti-LPG mAbs of different specificity, AP3, LT6, and WIC79.3. The binding of these mAbs indicates the presence of terminal mannooligosaccharides as well as unsubstituted and galactosylated phosphodisaccharides in PPG. Fractions of *peak A* were pooled, and PPG was recovered by ultrafiltration (Fig. 1*A, lane 5*). A second phosphate peak (Fig. 2, *peak B*) not reactive in two-site ELISA was found near the elution position of the 80-kDa marker protein. On SDS-PAGE, pooled fractions of *peak B* showed a broad Stains-all-stained area between 50 and 10 kDa apparent molecular mass (Fig. 1*A, lane 8*) which is typical for LPG and PG. Monosaccharide analysis of these fractions yielded Man, Gal, Gal-6-PO_4, and Ara (not shown). It is therefore likely that peak B corresponds to PG (34) recently characterized in *Leishmania donovani* (35), and it was not further analyzed. After ultracentrifugation of PPG-containing octyl-Sepharose eluates in the presence of CsCl (see above), PG remained in the supernatant and peak B was not observed in subsequent Superose 6 chromatography (not shown, compare Fig. 9*A*). Quantities of PPG larger than 200 μg could not be processed by Superose 6 chromatography, because the high viscosity of PPG solutions exceeding about 1 mg/ml led to loss of resolution and extensive backpressure. PPG at a concentration above 10 mg/ml formed a gel, a property not observed for either PG or LPG at even higher concentrations.[2] Therefore, ultracentrifugation in the presence of CsCl was the method of choice for the purification of larger amounts of PPG. One liter of culture supernatant from densely grown *L. major* promastigotes (>10^8/ml) yielded 5–10 mg of PPG (compare Table I).

TABLE I
Purification of L. major PPG

	Total protein	Total PO_4[a]	PO_4/ protein	Purification factor[b]
	mg	*mg*		
Culture supernatant	3366.0	17.6	0.005	1
DE52-cellulose eluate	23.25	7.20	0.31	62
Octyl-Sepharose eluate	0.412	6.27	15.2	3004
Ultracentrifugation in CsCl	0.075	3.13	41.7	8347

[a] PO_4-associated with *Leishmania*-derived macromolecules >3 kDa.
[b] Based on the PO_4/protein ratio.

The different stages of PPG purification were also monitored on immunoblots with the anti-LPG-mAb WIC108.3, which binds to the network-forming antigens secreted by *L. major* promastigotes (37). The Stains-all-stained material in the SDS-PAGE stacking gel, which was enriched during the purification procedure (Fig. 1*A, lanes 3–6*), strongly reacted with this mAb (Fig. 1*B, lanes 1–4*).

Both purification procedures resulted in a final product free from protein and LPG/PG contamination, as judged by several criteria. 1) Silver staining of overloaded SDS-polyacrylamide gels did not reveal any bands other than the broad area occupied by PPG in the stacking gel (Fig. 1*A, lane 7*). 2) Extensive biotinylation under alkaline conditions favoring lysine modification, pH 9.5, followed by SDS-PAGE, blotting, and detection of biotinylated products by enzyme-labeled avidin led only to the detection of PPG (Fig. 1*B, lane 6*). Since large amounts of biotinylated PPG with a very low lysine content (less than 0.8 mol %, see Table II) in comparison with potential contaminating proteins (average lysine content of 6–7 mol % (38)) were loaded, a high level of protein contamination is unlikely. 3) Both Stains-all staining after SDS-PAGE and immunodetection on blots by WIC108.3 failed to detect LPG- or PG-like compounds in the final product (Fig. 1*A*, compare *lanes 5–8;* Fig. 1*B*, compare *lanes 3–5*).

Purified PPG contains large amounts of phosphate, whereas its protein content determined by the Coomassie Blue dye binding assay is very low (Table I). Based on the PO_4/protein ratio, an overall purification factor for PPG of more than 8,000 was calculated (Table I).

Compositional Analysis—L. major PPG contains 4.4% amino acids, 20% phosphate (PO_4), and 75.6% monosaccharides (w/w). Monosaccharide analysis of native PPG yielded Man, Gal, and Gal-6-phosphate as well as small amounts of Ara and Glc (Table II). To quantitate the ratio of hexoses in PPG, it was dephosphorylated by HF prior to sugar analysis. The ratio of Man to Gal was 1:1.1. PPG did not contain detectable amounts of GlcNAc, GalNAc, or *myo*-inositol.

To confirm the presence of a protein backbone, PPG was incubated with various proteinases, and the products were subjected to SDS-PAGE and agarose gel electrophoresis.

[2] T. Ilg, unpublished results.

TABLE II
Monosaccharide analysis of L. major PPG

Monosaccharide	HF/ trifluoroacetic acid/ alditol acetates	Methanolysis/ trimethylsilylation diazomethane treatment	High pH anion exchange HPLC
	mol/mol	*mol/mol*	*mol/mol*[a]
Mannose	62[b]	62[b]	62[b]
Galactose-6-PO_4		+[c]	52
Galactose	68	27	19
Glucose	1	2	
Arabinose	1	1.5	1

[a] Calculated from the relative abundance of PPG glycans (Table V).
[b] Normalized to 62 mannose.
[c] Present but not quantitated.

Stains-all staining patterns of the PPG proteinase digestion products on SDS-PAGE were indistinguishable from native PPG even on 4% acrylamide gels (not shown). However, on agarose gels, proteinase K and thermolysin digestion led to an increased mobility of PPG (Fig. 3, compare *lanes 1–3*). To a lesser degree, a mobility shift could also be detected after trypsin (Fig. 3, *lane 4*), papain, and chymotrypsin digestion (not shown).

Amino acid analysis of PPG revealed a highly unusual composition dominated by three amino acids, Ser (>50 mol %), Ala, and Pro, which together represent more than 87 mol % of the protein backbone(s) residues of *L. major* PPG (Table III).

Deglycosylation of PPG and Structural Analysis of Mild Acid-released Glycans—PPG was hydrolyzed by HCl under mild conditions that preferentially hydrolyze hexose-1-PO_4 linkages, whereas glycosidic linkages remain intact (5, 6, 28). Under these conditions, the carbohydrate was quantitatively (>99.8%) released as low molecular mass (<3000 Da) neutral and phosphorylated oligosaccharides. Alternatively, PPG was subjected to HF dephosphorylation that also released >99.5% of the carbohydrates as neutral glycans with HPLC peak patterns identical to that of mild acid-released and enzymatically dephosphorylated PPG glycans (not shown). The mild acid-released glycans of *L. major* PPG were separated by high pH anion exchange HPLC by a salt program that resolves both neutral and phosphorylated oligosaccharides. Three neutral (N2, N2′, N3) and four phosphorylated glycans (P2, P3, P4a, P4b) were detected (Fig. 4*A*). N2 and N2′ co-eluted on anion exchange HPLC with Galβ1–4Man and Manα1–2Man, respectively, which had been previously identified as cap structures in various *Leishmania* LPGs (8–12) and *L. mexicana* sAP (18). Methylation analysis (Table IV) and compositional analysis (not shown) were consistent with these structures. The anomeric configurations were confirmed by their susceptibility to β-galactosidase and α-mannosidase treatment, respectively. N3 contained Gal and Man in the ratio of 2:1. Methylation analysis (Table IV) and the degradation of N3 by β-galactosidase to monosaccharides suggests the structure Galβ1–3Galβ1–4Man. This is corroborated by the co-elution of N3 with dephosphorylated P3 isolated from *L. major* LPG. In the case of the phosphorylated oligosaccharides, the detection of Gal-6-PO_4 as the only phosphorylated monosaccharide, the results of methylation analysis of P2, P3, P4a, and P4b after enzymatic dephosphorylation, and co-elution on HPLC with their previously characterized counterparts isolated from *L. major* LPG (Fig. 4, *A* and *B*) (7, 8) indicate the structures PO_4-6-Galβ1–4Man (P2), PO_4-6(Galβ1–3)Galβ1–4Man (P3), PO_4-6(Araβ1–2Galβ1–3)Galβ1–4Man (P4a), and PO_4-6(Galβ1–3Galβ1–3)Galβ1–4Man (P4b), respectively. The hydrolysis of dephosphorylated P2, P3, and P4b to monosaccharides by β-galactosidase confirms the anomeric configuration of their Gal residues and the carbohydrate sequence, whereas the resistance of P4a to this enzyme is in agreement with a terminal Ara capping the oligosaccharide.

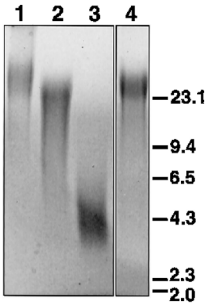

FIG. 3. **Agarose gel electrophoresis (0.6%) of proteinase-treated *L. major* PPG.** *Lane 1*, PPG (10 μg); *lane 2*, proteinase K-treated PPG (10 μg); *lane 3*, thermolysin-treated PPG (10 μg); *lane 4*, trypsin-treated PPG (10 μg); λ-phage DNA digested with the restriction enzyme *Hin*dIII was used as a reference. The molecular mass of the DNA fragments is indicated in kilobase pairs.

TABLE III
Amino acid analysis (mol %) of L. major PPG

Amino acid	Native PPG[a]	PPG after reduction and alkylation[d]	PPG after thermolysin digestion[b,c]	PPG/mild acid, soluble fraction[c]	PPG/mild acid, insoluble fraction[c]
Asx	1.7 ± 0.3	1.7	0.75 ± 0.1	0.5 ± 0	9.2 ± 0.2
Thr	1.4 ± 0.1	1.2	0.5 ± 0	0.5 ± 0	6.5 ± 0.1
Ser	51.8 ± 1.4	51.0	58.95 ± 0.5	58.6 ± 0.1	11.6 ± 0.2
Glx	1.7 ± 0.3	1.55	0.4	0.0	10.1 ± 0.5
Pro	14.4 ± 0.5	14.6	15.3 ± 0.1	16.0 ± 0	6.2 ± 0
Gly	1.5 ± 0.2	1.4	0.6 ± 0.3	0.6 ± 0.1	8.0 ± 0.3
Ala	21.25 ± 0.7	21.6	23.15 ± 0.2	23.4 ± 0	9.8 ± 0.2
Val	1.2 ± 0.2	1.1	0.0	0.0	5.6 ± 0.6
Met	0.25 ± 0.2[e]	0.3	0.0	0.0	2.1 ± 0
Ile	0.6 ± 0.1	0.8	0.0	0.0	3.35 ± 0.5
Leu	1.9 ± 0.2	2.2	0.35 ± 0.1	0.4 ± 0	9.9 ± 0.3
Tyr	0.4 ± 0.3[e]	0	0.0	0.0	3.7 ± 0.3
Phe	0.4 ± 0.4[e]	0.6	0.0	0.0	3.9 ± 0.3
His	0.2 ± 0.2[e]	0.4	0.0	0.0	1.65 ± 0
Lys	0.7 ± 0.1	(0.85)[c]	0.0	0.0	4.2 ± 0.2
Arg	0.5 ± 0.5[e]	0.7	0.0	0.0	4.3 ± 0.1

[a] Average of three determinations.
[b] PPG was repurified by Superose 6 chromatography in the presence of 6 M GdmCl.
[c] Average of two determinations.
The standard deviations are indicated.
[d] Coelution of lysine and *S*-pyridylethylocysteine.
[e] High standard deviation caused by 0 readings in one of the analyses, respectively.

Methylation analysis of HF-treated unfractionated PPG glycans yielded the same derivatives as shown in Table IV. No 3,6-linked Man was detected, which together with the absence of GlcNAc indicates that *N*-linked glycans, if present, are of low abundance. The small amount of Glc detected in the compositional analysis (Table II) is most likely due to contaminants, since no corresponding glycan structure could be identified from high pH anion exchange HPLC.

^{1}H and ^{31}P NMR Spectroscopy of Native PPG—The anomeric proton region of the one-dimensional ^{1}H NMR spectrum of native PPG is shown in Fig. 5*A*. The various signals were assigned on the basis of $J_{1,2}$ coupling constants, heteronuclear J_{HP} couplings, chemical shifts, and comparisons with previously reported NMR data (5, 7, 18, 39). The doublet at 5.68 ppm (J_{HP} ~8 Hz) corresponds to the shift for the H-1 proton of Manα1-PO_4 substituted at the 2-position with α-Man (18). The anomeric signal of the terminal α-Man linked to this residue appears as a well resolved peak at 5.05 ppm with a matching integral (Fig. 5*A*) to the peak at 5.68 ppm. The assignment of both residues has been confirmed by two-dimensional TOCSY. The intense overlapping doublet signals at 5.44 ppm correspond to 4-linked Manα1-PO_4 (5, 7). The small doublet upfield

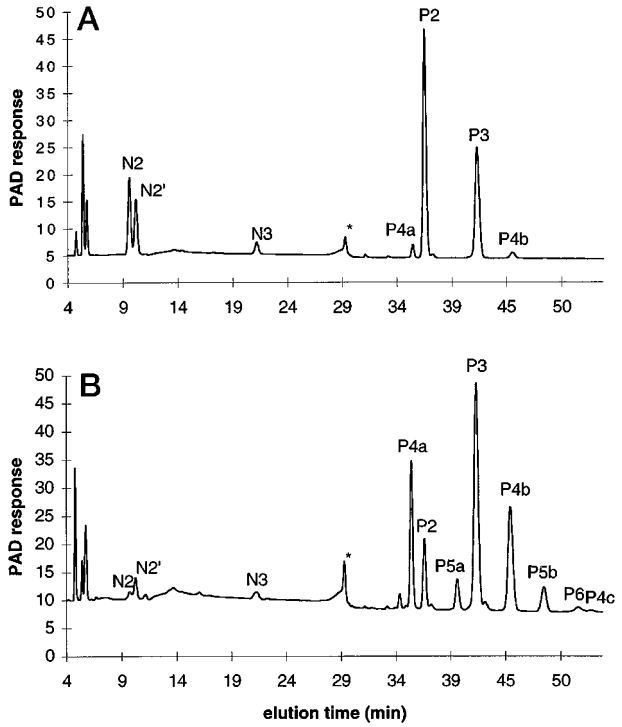

FIG. 4. **High pH anion exchange HPLC profiles of *L. major* PPG and LPG glycans released by mild acid hydrolysis.** Neutral (*N*) and phosphorylated (*P*) glycans from mild acid-treated *L. major* PPG (*A*) and LPG (*B*) were resolved on a Carbo-Pac PA1 column as described under "Experimental Procedures." The nomenclature is derived from LPG (7). * is a spike corresponding to the change in the gradient.

of this peak is assigned as H-1 of terminal $Ara_p\beta1–2$ based on the similarity of the H-1 (5.36 ppm) and H-2 (3.86 ppm, determined from a TOCSY spectrum, not shown) chemical shifts to those of the corresponding dephosphorylated oligosaccharide from *L. major* LPG (7, 8). The doublet at 4.64 ppm shows a chemical shift and large coupling constants ($J_{1,2}$ ~7.8 Hz) corresponding to Gal in a β-configuration. Its corresponding H-2 shift was determined to be 3.63 ppm from a DQFCOSY spectrum (not shown), and it is assigned as arising from a terminal Galβ1-linked to the 3-position of an adjacent sugar residue. Linkage of Galβ- to the 4-position rather than the 3-position of the adjacent residue results in an upfield shift for both H-1 and H-2. A cross-peak in the DQFCOSY spectrum between 4.46 and 3.55 ppm thus allowed the H-1 doublet ($J_{1,2}$ ~7.8 Hz) at 4.46 ppm to be assigned to a terminal Galβ1–4. The overlapped multiplet at 4.54 ppm was assigned to 3-linked PO_4-6-Galβ1–4 since the DQFCOSY spectrum showed that the shifts of H-2 (3.71 ppm), H-3 (3.87 ppm), and H-4 (4.25 ppm) were almost identical to those of the corresponding residues in LPG (7). Finally, the doublet at 4.48 ppm (partially overlapped with the doublet at 4.46 ppm) was assigned to H-1 of the PO_4-6-Galβ1–4 moiety. These results are consistent with the proposed structures for the mild acid-released glycans (Table V). ^{31}P NMR spectroscopy of PPG in D_2O at pH 7.5 resulted in a single peak envelope (Fig. 5*B*). A non-Lorentzian peak shape, however, suggested a superposition of several different ^{31}P nuclei. The chemical shift of the peak envelope is consistent with PO_4 in phosphodiester bonds. Titration experiments (pH 3.1–9.2) resulted in virtually no change (within 0.05 ppm) in chemical shift, corroborating a phosphodiester environment for the ^{31}P nuclei. In contrast, ^{31}P resonance signals of phosphomonoesters in proteins are expected to have different and pH-dependent chemical shifts (40), as demonstrated on the phosphoprotein phosvitin (not shown). Based on the intensity of the phosphodiester signal and the base-line noise level, phosphomonoester, if present, would account for less than 2% of the PO_4 detected in PPG.

To resolve the overlapping ^{31}P NMR peaks a HMBC spectrum (41) of PPG in D_2O was recorded. This shows only protons having a long range spin-spin coupling interaction with ^{31}P nuclei. A major advantage of this two-dimensional technique is the resolution of partially overlapping ^{31}P NMR signals by differing chemical shifts of ^{1}H resonance signals. Three signals are detected in the two-dimensional contour plot (Fig. 5*C*). The two well resolved signals in the downfield region correspond to a 2-linked Manα1-O-P and a 4-linked Manα1-O-P with ^{1}H chemical shifts of 5.68 and 5.44 ppm, respectively. The signal at 4.06 ppm falls in a crowded region of the ^{1}H spectrum. Initially, it was believed that it corresponded to the linkages P-O-6-C$\underline{H}_2$-Gal and P-O-C$\underline{H}_2$-Ser, which are both abundant in PPG (Table II and see below Fig. 6*A*). HMBC experiments with authentic Ser(P) and Gal-6-PO_4 confirmed that both types of CH_2/P-correlations were detectable and that the ^{1}H chemical shifts of the CH_2 groups of both compounds occurred in this region of the ^{1}H spectrum. However, subsequent HMBC spectra on phosvitin, which contains abundant P-O-CH_2-Ser linkages, did not produce cross-peaks in HMBC spectra, despite their detection in Ser(P) itself. The difficulty in detecting the latter linkage in the intact PPG (and phosvitin) is likely due to the relatively high degree of immobilization of the P-O-CH_2-Ser moiety in these proteins. The resultant fast T_2 relaxation leads to loss of magnetization in the HMBC experiment for this linkage, whereas the more mobile P-O-6-CH_2-Gal linkage is readily detected. It therefore appears that the upfield signal at 4.06 ppm in Fig. 5*C* may be due to P-O-6-CH_2-Gal alone.[3] These data provide direct evidence for the presence of the sequence 4-Manα1-PO_4-6Gal in PPG. Interestingly, no Gal-6-PO_4 peak appears at the ^{31}P shift of the 2-linked Manα1-PO_4. A possible explanation could be that Manα1–2Manα1-PO_4 is predominantly directly linked to the "HMBC-invisible" Ser and not to 6-Gal.

Comparison of the Glycans from PPG and LPG Purified from the Same Parasite Culture—The ratios of the different neutral and phosphorylated PPG glycans were determined by high pH anion exchange HPLC (11, 18). The molar ratios of Man, Gal, Gal-6-PO_4, and Ara in *L. major* PPG calculated from peak integration of the PPG oligosaccharides are consistent with the results obtained by monosaccharide analysis (see Table II). The dominating structures in PPG are P2 and P3 followed by N2 and N2′, whereas N3, P4a, and P4b are only minor components (Table V). In LPG purified from the parasite cell pellet grown in the culture supernatant used for PPG isolation, all the PPG oligosaccharides are also detected. However, P3 and P4b followed by P4a are the dominant structures in LPG, whereas P2, by far the most abundant structure in PPG, is only a minor component in LPG (Fig. 4*B* and Table V). LPG contains additional, more highly substituted phospho-oligosaccharides (P5a, P5b, P6, and P4c, (7), see Fig. 4*B*), which were not detected in PPG. The average ratio of phosphorylated oligosaccharides to neutral oligosaccharides is 18.6:1 in the case of LPG and 3:1 in PPG (Table V).

PPG Glycans Are Linked to Ser(P) via Phosphodiester Bonds—Mild acid hydrolysis and aqueous HF treatment re-

[3] Evidence for this difference in mobility was obtained from ^{31}P spectra recorded on phosvitin. Its half-height line widths are 5-fold greater than the respective line width for PPG in Fig. 5*B*. Close inspection of the PPG signal reveals that the peak contains a broad component near the base. Possibly the sharp part of the peak arises from mobile P-O-6-CH_2-Gal linkages and the broad component from P-O-CH_2-Ser linkages.

TABLE IV
Methylation analysis of the L. major PPG oligosaccharides

Deduced glycosidic linkage	N2[b]	N2′ (+N2)[a,b]	N3[c]	P2[a]	P3[c]	P4a (+P2)[a,b]	P4b[c]
t-Ara$_p$	0	0	0	0	0	1.0	0
t-Gal$_p$	1.1		1.1	1.2	1.1		1.0
		(1.1)				*(0.6)*	
t-Man$_p$	0	0.6	0	0	0	0	0
2-Man$_p$	0	0.6	0	0	0	0	0
4-Man$_p$	1.0		1.0	1.0	1.0	1.4	1.0
		(1.0)				*(0.6)*	
2-Gal$_p$	0	0	0	0	0	1.5	0
3-Gal$_p$	0	0	0.8	0	1.05	1.2	1.9

[a] GC-MS on a BP×70 column.
[b] N2′- and P4a isolated by high pH anion exchange HPLC contained small amounts of N2 and P2, respectively. The PMAAs derived from these contaminants are depicted in italics.
[c] GC-MS on a cpsil5 column.

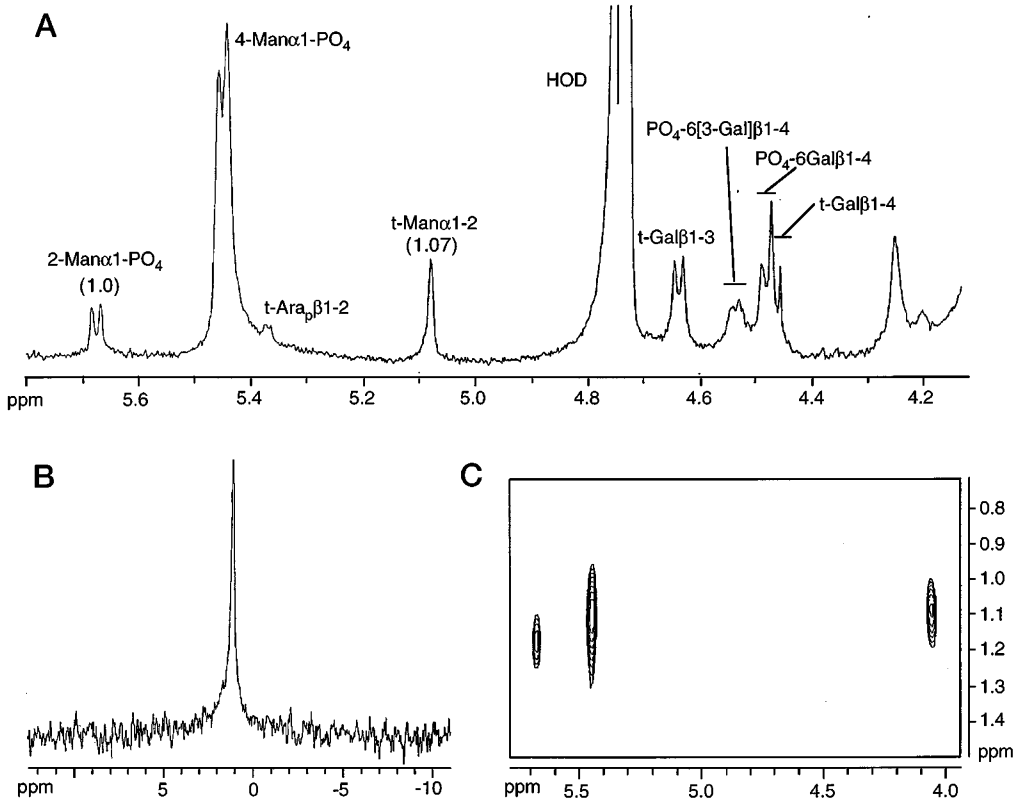

FIG. 5. **NMR spectroscopy of native *L. major* PPG.** *A*, anomeric region of the 500 MHz ^{1}H NMR spectrum of PPG in D_2O. Some of the relative peak integrals are shown in parentheses under the assignment. *B*, ^{31}P NMR spectrum of PPG. *C*, HMBC spectrum of PPG. The cross-peaks connect phosphorus nuclei with spin-coupled protons.

leased almost quantitatively the PPG glycans from the protein backbone (see above). Since these hydrolysis conditions do not cleave glycosidic bonds (5, 6, 29, 42, 44), it is likely that all the glycans were linked to the protein by mild acid- and HF-labile phosphodiesters similar to the main glycans in *L. mexicana* sAP (18) and not by *N*- or *O*-glycosidic linkages. Phosphoamino acid analysis of the PPG protein backbone indicated the presence of large amounts of Ser(P) (Fig. 6*A*). No phosphothreonine or phosphotyrosine was detected. Ser(P) in PPG was not susceptible to alkaline phosphatase treatment (Fig. 7). Heating prior to alkaline phosphatase addition or removal of all the glycans by mild acid hydrolysis alone did not have an impact on the Ser(P) content of PPG. However, a combination of mild acid hydrolysis and alkaline phosphatase treatment resulted in the complete enzymatic dephosphorylation of PPG-associated Ser(P) (Fig. 7). Phosvitin, a highly phosphorylated egg yolk protein containing up to 100 Ser(P) residues (43), was completely dephosphorylated by alkaline phosphatase without any pretreatment, which demonstrates that protein-bound, clustered Ser(P) is not inherently resistant to enzymatic dephosphorylation (Fig. 7). These experiments indicate that all the Ser(P) residues in PPG are in mild acid-labile phosphodiester bonds with glycans, consistent with the results of the ^{31}P NMR experiments on intact PPG (see above). Based on the degree of Ser(P) hydrolysis to Ser and phosphate under the partial acid hydrolysis conditions (30.6%, Fig. 6*B*) and the relative response factors of Ser(P) and serine as phenylthiocarbamyl derivatives (1:1.09), the degree of Ser phosphorylation in native PPG was estimated to be 84%. Therefore, Ser(P) linked to phosphoglycans and/or neutral glycans accounts for at least 43 mol % of the amino acids in the polypeptide backbone of PPG.

Fragmentation of the PPG Polypeptide Backbone by Mild Acid Hydrolysis—The selectivity of mild acid hydrolysis for hexose 1-phosphate linkages in phosphoglycans has been well

TABLE V
Structure and relative abundance of oligosaccharides released from L. major PPG and LPG by mild acid hydrolysis

Oligosaccharide	Structure	PPG	LPG[a]
		mol %	
N2	Galβ1–4Man	13.0	1.0
N2′	Manα1–2Man	9.5	2.7
N3	Galβ1–3Galβ1–4Man	2.5	1.4
P2	PO_4-6Galβ1–4Man	43.0	8.6
P3	PO_4-6[Galβ1–3]Galβ1–4Man	28.5	39.0
P4a	PO_4-6[Araβ1–2Galβ1–3]Galβ1–4Man	2.0	16.2
P4b	PO_4-6[Galβ1–3]$_2$Galβ1–4Man	1.5	20.9
P4c	PO_4-6[Glcβ1–3Galβ1–3]Galβ1–4Man	ND[a]	0.2
P5a	PO_4-6[Araβ1–2Galβ1–3Galβ1–3]Galβ1–4Man	ND[a]	4.4
P5b	PO_4-6[Galβ1–3]$_3$Galβ1–4Man	ND[a]	4.8
P6	PO_4-6[Galβ1–3]$_4$Galβ1–4Man	ND[a]	0.8
Ratio of phosphorylated glycans to neutral glycans		3.0:1	18.6:1

[a] For the structural analysis of LPG cap oligosaccharides and phosphooligosaccharides and the assignment of their peaks see McConville *et al.* (7, 8, 11): ND = not detected.

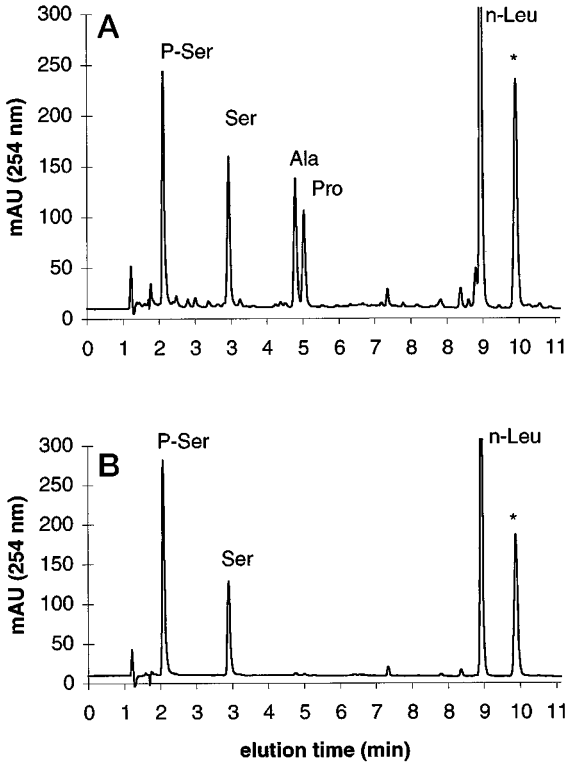

FIG. 6. **Reversed phase-HPLC of amino acids and phosphoamino acids.** *L. major* PPG (*A*) and Ser(P) (*B*) were subjected to partial acid hydrolysis (6 M HCl, 90 min, 110 °C), converted to their respective phenylthiocarbamyl derivatives, and resolved on a Pico-Tag column. Norleucine (*n-Leu*) was added as an internal standard. * represents the reagent peak.

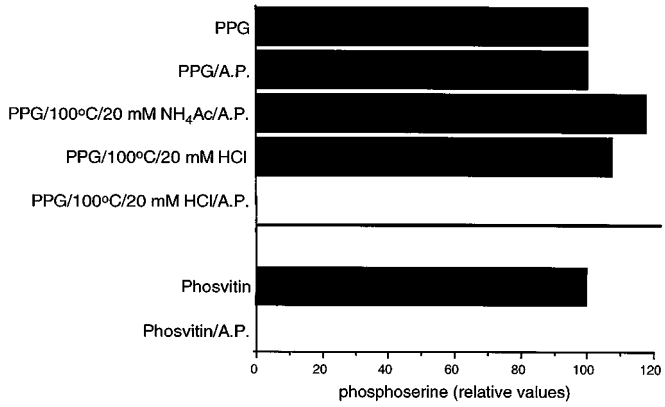

FIG. 7. **Susceptibility of protein-bound Ser(P) to alkaline phosphatase.** The Ser(P) content of PPG was analyzed without pretreatment (*PPG*) or after alkaline phosphatase digestion (*PPG/A.P.*), control treatment in 20 mM NH_4acetate followed by alkaline phosphatase digestion (*PPG/100 °C/20 mM* NH_4*Ac/A.P.*), cleavage of hexose1-PO_4 linkages by mild acid hydrolysis (*PPG/100 °C/20 mM* HCl), and cleavage of hexose 1-PO_4 linkages followed by alkaline phosphatase digestion (*PPG/100 °C/20 mM* HCl/A.P.). Phosvitin served as a control and was analyzed before (*phosvitin*) and after alkaline phosphatase (*phosvitin/A.P.*) digestion.

established (5–7, 28, 42). In contrast, its effect on peptide bonds has not been described. Bovine serum albumin (BSA) and phosvitin were used as model proteins and subjected to mild acid hydrolysis. Both BSA and especially phosvitin were cleaved into a large array or smear of smaller polypeptides as indicated by their higher mobilities in SDS-PAGE (Fig. 8, *lanes 1–4*). Similarly, mild acid hydrolysis of PPG led to a broad area of hydrolysis products spanning an area from an apparent molecular mass of 90 kDa to the dye front of the gel (Fig. 8, *lane 5*). This broad staining pattern is not due to the released phosphoglycans, which migrate at the front of the gel (37). Protein sequencing of intact PPG did not yield any amino acids indicating a blocked N terminus, whereas after mild acid hydrolysis Ser, Ala, and Pro were detected as N-terminal residues. This result provides further evidence for peptide bond cleavage in PPG during mild acid deglycosylation. When large amounts of PPG (>500 μg) were subjected to mild acid hydrolysis, the formation of a precipitate was observed. This precipitate was insoluble in nondenaturing aqueous buffers and could be recovered as a pellet after centrifugation. The washed pellet fraction and the combined supernatants were subjected to amino acid analysis (Table III). The pellet fraction contained only about 5% of the amino acids; it was greatly depleted for Ser, Ala, and Pro and showed increased readings for all other amino acids proportional to their previous abundance in intact PPG. On SDS-polyacrylamide gels, this minor peptide fraction gave rise to a broad area spanning from approximately 90 to 40 kDa apparent molecular mass (Fig. 8, *lane 6*). About 95% of the amino acids were recovered in the mild acid hydrolysis supernatant. This soluble fraction was strongly enriched for Ser, Ala, and Pro, which accounted for 98 mol % of its amino acids (Table III). On SDS-PAGE this fraction was indistinguishable from the total hydrolysate (Fig. 8, compare *lanes 5* and *7*).

Based on these observations, two different approaches were chosen to obtain antisera against the deglycosylated protein backbone of PPG. 1) The insoluble peptide pellet of mild acid-hydrolyzed PPG was used for the immunization of rabbits, which yielded an antiserum directed against mild acid-insoluble peptides of PPG (anti-MIP serum). 2) Since the soluble fraction contains more than 58% serine (Table III), the presence of long polyserine stretches in the polypeptide backbone

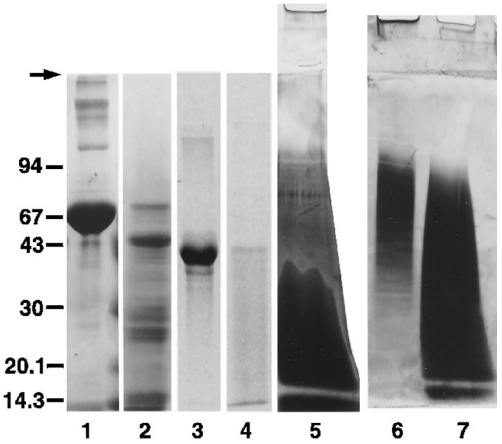

FIG. 8. **SDS-PAGE of bovine serum albumin (BSA), phosvitin, and *L. major* PPG after mild acid hydrolysis.** *Lane 1*, BSA (25 μg); *lane 2*, BSA (25 μg), after mild acid hydrolysis; *lane 3*, phosvitin (25 μg); *lane 4*, phosvitin (25 μg) after mild acid hydrolysis; *lane 5*, PPG (25 μg), after mild acid hydrolysis; *lane 6*, PPG (500 μg), after mild acid hydrolysis, insoluble peptide fraction; *lane 7*, PPG (25 μg), after mild acid hydrolysis, soluble peptide fraction. The boundary of stacking and separating gel is marked by an *arrow*. The positions of standard proteins and their molecular mass in kDa are indicated.

was considered likely, and antisera against synthetic polyserine were raised in rabbits (anti-PS serum).

Gel Filtration Chromatography of Native, Reduced, and Alkylated and Thermolysin-treated PPG in the Presence of 6 M GdmCl—PPG chromatographed on Superose 6 equilibrated in 6 M GdmCl to minimize aggregation showed a co-eluting peak of phosphate and material absorbing at 280 nm. In dot blots the PPG peak fractions were strongly recognized by the anti-MIP and anti-PS antisera (Fig. 9*A*). The elution position of PPG was similar to that observed in 250 mM ammonium acetate and suggested an apparent molecular mass of more than 2000 kDa also under dissociating conditions. Reduction and alkylation of PPG with either iodoacetamide or vinylpyridine did not result in any change in its elution position on Superose 6 (not shown), and its amino acid composition was nearly identical to that of native PPG (Table III). Thermolysin treatment leads to higher mobility of PPG on agarose gels indicative of some peptide bond cleavage (Fig. 3). On Superose 6, however, the majority of the phosphate (>90%) of thermolysin-digested PPG still eluted near the void volume, but the absorbance at 280 nm of these fractions was greatly diminished compared with the native PPG. Peak fractions reacted on dot blots strongly with the anti-phosphoglycan mAb WIC108.3 but more weakly with anti-MIP serum (Fig. 9*B*). Amino acid analysis of pooled peak fractions showed a composition highly enriched for Ser, Ala, and Pro (together >97 mol %), virtually identical to the composition of the soluble peptide fraction of mild acid-hydrolyzed PPG (Table III). These results indicate that while parts of PPG may be susceptible to thermolysin, the molecule also contains large highly glycosylated and phosphorylated polypeptide regions consisting almost exclusively of Ser, Ala, and Pro, which are resistant to proteinases.

Analysis of the PPG Polypeptide Backbone after Aqueous HF Treatment—PPG was dephosphorylated and deglycosylated by aqueous HF treatment. The impact of aqueous HF on peptide bonds was tested on BSA, which was included as a control in each set of incubations. In contrast to mild acid hydrolysis, HF did not result in peptide bond cleavage detectable on SDS-PAGE (Fig. 10, *lanes 1* and *2*). HF treatment of PPG resulted in the formation of a protein precipitate. After solubilization by the addition of 6 M GdmCl and Superose 6 gel filtration, a single phosphate peak was detected near the inclusion volume, the

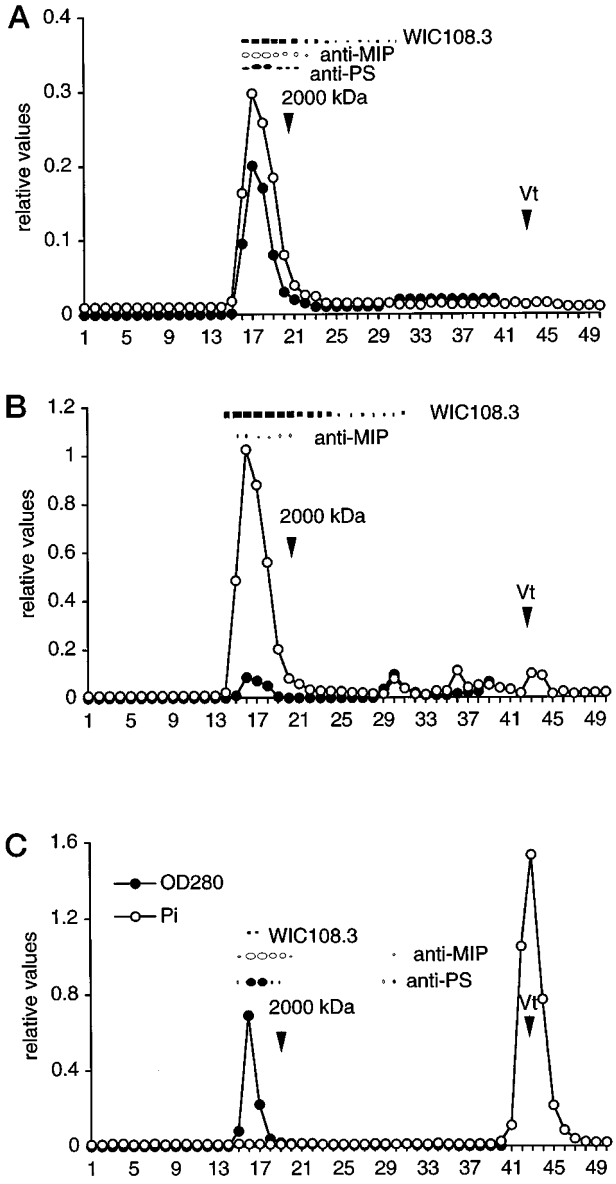

FIG. 9. **Gel filtration chromatography of GdmCl-denatured *L. major* PPG.** PPG (*A*), PPG after thermolysin treatment (*B*), and PPG after HF treatment (*C*) was chromatographed on Superose 6 in the presence of 6 M GdmCl. Fractions monitored for protein (OD_{280}) and phosphate (P_i). Aliquots (1 μl) of the fractions were spotted onto membranes and analyzed with mAb WIC108.3, the anti-MIP, and the anti-PS antisera. The reactive fractions are marked in the graph by *dots*. The elution position of dextran blue (2000 kDa) and the inclusion volume (V_t, CTP) are indicated.

expected position of free phosphate as a reaction product of HF dephosphorylation (Fig. 9*C*). In addition, a protein peak eluting earlier than the 2000-kDa marker compound was observed. Fractions collected over this protein peak strongly reacted with the anti-PS and the anti-MIP sera on dot blots, whereas reaction with anti-phosphoglycan mAb WIC108.3 was very weak or absent, as expected for a deglycosylated product (Fig. 9*C*). Therefore, it is likely that this protein peak corresponds to (part of) the polypeptide backbone of PPG. This is corroborated by amino acid analysis of peak fractions desalted by filtration onto polyvinylidene difluoride membrane supports, which showed a similar amino acid composition (>39% Ser, 15% Ala, 10% Pro) as native PPG. However, the elution close to the void volume, which was not altered by prior reduction (not shown), may indicate aggregation, even in the presence of GdmCl. The GdmCl-containing Superose 6 protein peak fractions of HF-

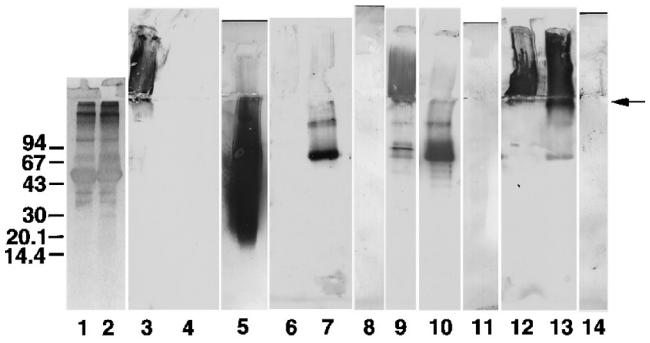

FIG. 10. **SDS-PAGE and SDS-PAGE immunoblot of native and HF-dephosphorylated/deglycosylated *L. major* PPG, LPG, and BSA.** *Lane 1*, BSA (20 μg); *lane 2*, HF-treated BSA (20 μg); *lanes 3, 6, 9, 12*, PPG (10 μg); *lanes 4, 7, 10, 13*, HF-treated PPG (10 μg); *lanes 5, 8, 11, 14*, LPG (5 μg). *Lanes 1* and *2* were stained with silver; *lanes 3–14* were blotted onto nitrocellulose and probed with mAb WIC108.3 (*lanes 3–5*), anti-PS serum (*lanes 6–8*), anti-MIP serum (*lanes 9–11*), and anti-HFP serum (*lanes 12–14*). The boundary of stacking and separating gel is marked by an *arrow*. For *lanes 3–14*, the positions of standard proteins and their molecular mass in kDa is indicated. In *lanes 1* and *2* the position of the major BSA band (molecular mass, 67 kDa) is offset from the position of the standards, because of the use of a shorter stacking and a longer separating gel than in the other lanes.

treated PPG were used to raise polyclonal antibodies against the dephosphorylated and deglycosylated polypeptide backbone of PPG (anti-HFP serum).

Native and HF-treated PPG were subjected to SDS-PAGE and immunoblotting using the PPG/LPG glycan-specific mAb WIC108.3 as well as the anti-PS, anti-MIP, and anti-HFP serum as detecting reagents. Native PPG migrating mainly in the stacking region of SDS-polyacrylamide gels was strongly recognized by mAb WIC108.3, the anti-MIP, and the anti-HFP serum (Fig. 10, *lanes 3, 9,* and *12*), whereas its reaction with anti-PS serum was weak (Fig. 10, *lane 6*). Some additional weak bands between the 94- and the 43-kDa marker protein (Fig. 10, *lanes 3, 9,* and *12*) may correspond to small amounts of degradation products. After HF treatment, PPG did not react with WIC108.3 (Fig. 10, *lane 4*), whereas the anti-PS, the anti-MIP, and the anti-HFP serum recognized protein bands near the position of the 67-kDa and above the 94-kDa marker protein (Fig. 10, *lanes 7, 10,* and *13*). In addition all three antisera, especially the anti-HFP serum, reacted with a smear in the stacking gel and the top of the separating gel, possibly aggregated PPG polypeptide(s). None of the antisera reacted with LPG (Fig. 10, *lanes 8, 11,* and *14*), which is strongly recognized by mAb WIC108.3 (Fig. 10, *lane 5*). This result indicates that the three antisera are predominantly directed against peptide epitopes of PPG and not against glycan determinants. The stronger reaction of PPG with anti-PS serum after HF dephosphorylation may reflect the unmasking of Ser-rich polypeptide regions previously covered by phosphoglycans.

Ultrastructure of Purified PPG—Inspection of purified *L. major* PPG by electron microscopy revealed long thread-like filaments with similar appearance after glycerol spraying and rotary shadowing (Fig. 11, *a* and *b*) as well as negative staining (Fig. 11*c*). The length of extended filaments is variable and can exceed 6 μm. The diameter of the majority of the PPG molecules appears to be homogeneous and may be around 3–6 nm. Occasionally thicker filaments with approximately twice this diameter were observed (Fig. 11*b*). Whether this subfraction is due to side by side-arranged filaments or corresponds to a distinct population of molecules remains to be determined. No evidence for branched structures has been found. The filaments exhibit high flexibility; they tend to curl up (Fig. 1, *A–C*) and can form large clumps on grids (not shown). These clumps were especially prevalent after labeling with monoclonal antibodies on grids, possibly due to cross-linking of flexible parts of the molecules not stably attached to the support (Fig. 11, *e* and *f*). PPG strands could be heavily labeled with the mAbs LT6, WIC79.3, AP3 (Fig. 11, *d–f*), and WIC108.3 (not shown), whereas a control antibody (LT8.2) showed very weak binding (Fig. 11*g*). These immunoelectron microscopy experiments confirm the modification of filamentous PPG by P2, P3/P4b, and N2′ at the ultrastructural level, since these glycans are part of the epitopes recognized by the mAbs.

DISCUSSION

Previous studies have shown that *Leishmania* promastigotes secrete network-forming filamentous material, which strongly reacts with anti-phosphoglycan antibodies (3, 20). *Leishmania* also secrete a phosphoglycan-modified acid phosphatase, which is organized as filaments in some species (17). In contrast to all other *Leishmania* species investigated so far, *L. major* does not secrete this enzyme (46), the presence of which complicates the isolation of this network component.[2] Therefore, *L. major* was chosen as the best source for the isolation of this antigen. Here we report the purification of this material from *L. major* promastigote culture supernatant by a combination of column chromatography and ultracentrifugation. The purification scheme takes advantage of the strong negative charge, the hydrophilicity, the large size, the rapid sedimentation, and the high buoyant density of this carbohydrate-rich secretory product. The ultrastructural and antigenic properties observed by electron microscopy suggest that it is closely related or identical to the network-forming material observed in promastigote cultures (20). The amount of PPG recovered by the purification procedure (5–10 mg/liter culture supernatant) is similar to the amount of LPG present on the surface of a corresponding number of promastigotes (12.2 mg/10^{11} cells) (47), which shows that it is a major parasite antigen. Compositional analysis indicates that the antigen is a highly unusual proteophosphoglycan (PPG). The majority of the mass of PPG is formed by Man, Gal, and phosphate, less than 5% (w/w) correspond to other sugars and amino acids. Structural analysis of the neutral (N2, N2′, N3) and phosphorylated (P2, P3, P4a, and P4b) *L. major* PPG glycans shows that they are identical to oligosaccharide structures of the cell surface LPG of *L. major* promastigotes (7, 11). N3, P3, P4a, and P4b linked to polypeptide have not been described and represent a novel protein glycosylation pattern, whereas N2, N2′, and P2 were detected as components of *L. mexicana* sAP (18). HMBC spectroscopy on native PPG demonstrates that the glycans are linked together by the basic structure R-Manα1-PO_4-6-Gal-R (see Fig. 12). The use of the HMBC technique is an important advance in the analysis of phosphoglycan-containing molecules, since it provides direct and unambiguous evidence for the connected ^{31}P and ^{1}H shifts of long range-coupled nuclei. Phosphodiester linkages to Ser(P), most likely by the basic structure R-Manα1-PO_4-Ser, anchor the PPG glycans to the polypeptide backbone (see Fig. 12). This new type of protein glycosylation has been recently described in *L. mexicana* sAP (18). The data suggest that this type of glycosylation accounts for the majority of the PPG glycans, and it appears unlikely that either the classical *O*-linked or *N*-linked glycans are present in PPG. There are three marked differences in the structural organization of the glycans in *L. major* PPG and LPG. 1) In PPG, multiple phosphoglycans are attached to a polypeptide backbone, whereas the glycolipid core of LPG carries only one repetitive phosphoglycan chain (7, 48). 2) The ratio of neutral cap oligosaccharides to phosphosaccharide repeats suggests, on average, shorter phosphoglycan chains on PPG compared with LPG (3 *versus* 18.6 repetitive units). 3) LPG contains a greater variety and more highly modified phosphosaccharide repeat units than PPG. The

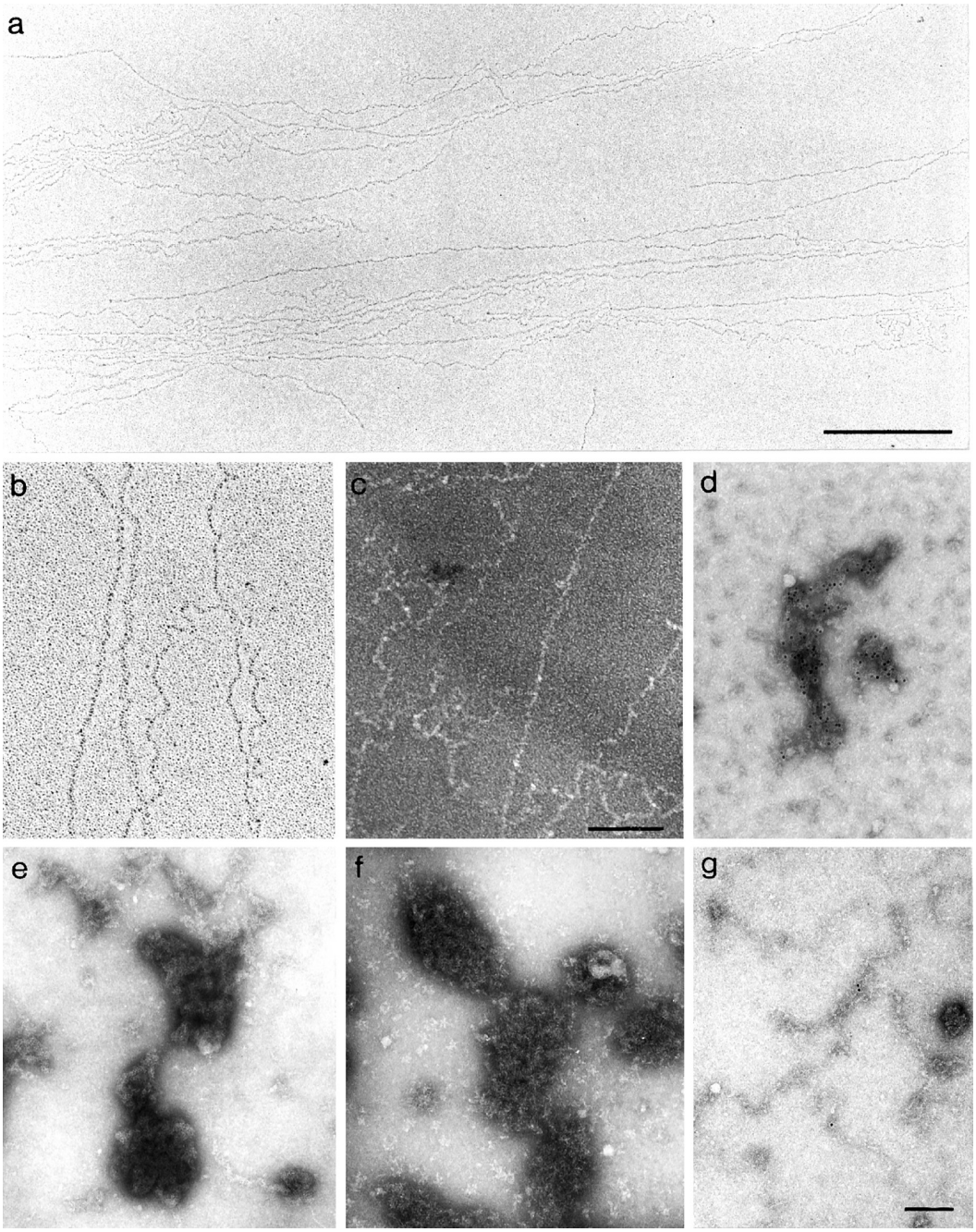

FIG. 11. **Electron microscopy and immunoelectron microscopy on purified *L. major* PPG.** *a*, strands of purified PPG after glycerol spraying and rotary shadowing. *b*, higher magnification detail showing strands of different diameter. *c*, negatively stained (Nano-W) PPG strands. *d–g*, immunolabeling of PPG strands and negative staining with uranyl acetate; *d*, mAb LT6 and protein A-6 nm gold, *e*, mAb WIC79.3; *f*, mAb AP3; *g*, control antibody (LT8.2) and protein A-6 nm gold. *Bars*: *a*, 500 nm; *b* and *c*, 100 nm; and *d–g*, 100 nm.

difference in average chain length between *L. major* PPG and LPG has also been observed for the protein- *versus* lipid-bound phosphoglycans in *L. mexicana* sAP and LPG, respectively. More than 95% of the cap glycans in *L. mexicana* sAP are (Manα1–2)$_{0-5}$Man. Therefore, on the assumption of a shared biosynthetic pathway, it has been proposed that a higher activity of the putative capping enzyme(s), the α1–2Man-transferase(s), on protein-bound *versus* lipid-bound phosphoglycan chains may lead to shorter phosphoglycan chains in sAP *versus* LPG (18). In the case of *L. major* PPG, however, more than 60% of the terminating neutral oligosaccharides are N2 and N3, the unphosphorylated counterparts of the repeats P2 and P3. They are more likely formed by ceasing phosphoglycan synthesis rather than specific capping events. The shorter phosphoglycan chains as well as the smaller amount and the more limited set of P2 modifications observed in *L. major* PPG compared with LPG may be explained by a preference of the enzymes responsible for phosphodisaccharide repeat backbone elongation (Manα1-PO$_4$-transferase(s) and β1–4Gal-transferase(s) (49, 50) and side chain modification (β1–3Gal-transferase(s) (51) and β1–2Ara-transferase(s)) for lipid-bound *versus* protein-bound acceptor sites. Alternatively, it is possible that the protein-bound phosphoglycans have shorter residence times in the biosynthetic compartment than their lipid-bound counterparts, which may limit the time necessary for the elongation of the repetitive phosphoglycan backbone and the synthesis of side chain modifications.

The composition of the *L. major* PPG polypeptide(s) is highly

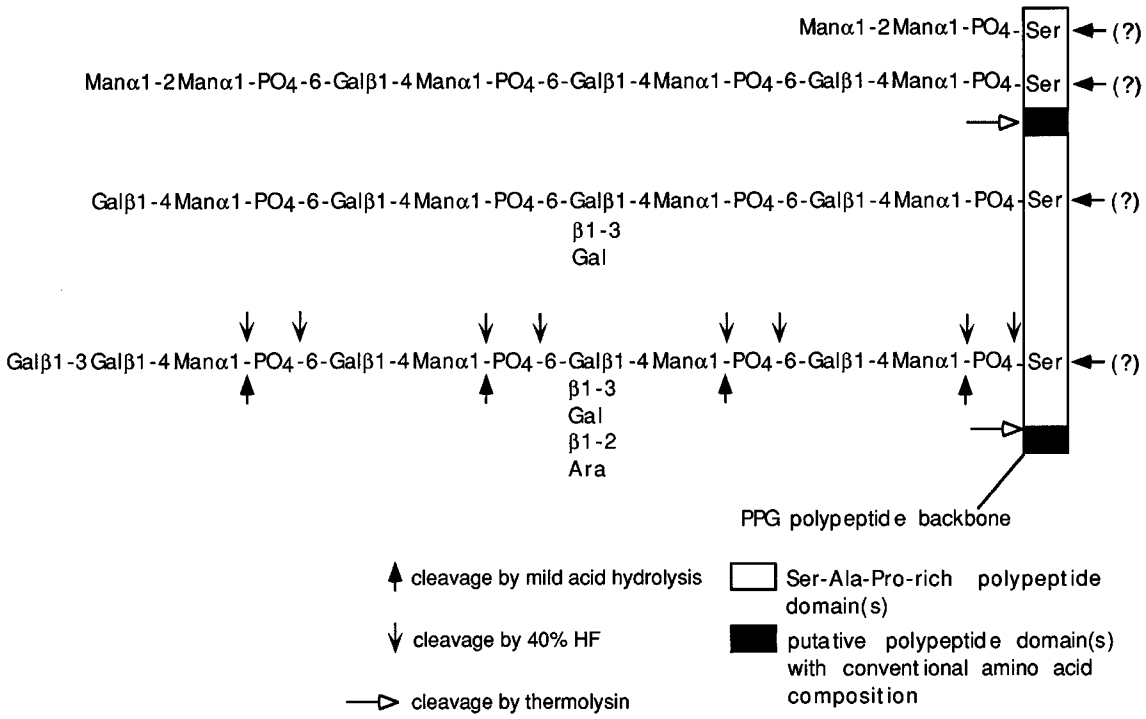

FIG. 12. **Schematic model for *L. major* PPG.** The structure of individual glycan chains as well as the relative arrangement and the number of the different polypeptide regions is unknown. (*?*) indicates putative peptide bond cleavage by mild acid hydrolysis.

unusual in being dominated by Ser, Ala, and Pro, which together account for about 87 mol % of the amino acids. More than 80% of the Ser residues are phosphorylated, which leads to a Ser(P) content of about 43 mol %. Only the egg yolk protein phosvitin (50–55 mol % Ser(P)) (43) and phosphophoryn, a structural protein identified in dentin of mammalian teeth (46 mol % Ser(P)) (52), are similarly Ser(P)-rich. However, in *L. major* PPG, all the Ser(P)) are in phosphodiester linkages to glycans, whereas both phosvitin and phosphophoryn contain Ser(P) exclusively in the nonglycosylated monoester form. Glycosylation of Ser(P) by single GlcNAc residues has been observed on a cysteine proteinase of *Dictyostelium discoideum* (45). More complex glycans and phosphoglycans modify Ser(P) on the sAP complex of *L. mexicana* promastigotes (18) and possibly also on a partially characterized proteophosphoglycan of *L. mexicana* amastigotes (53).

It is currently unclear if *L. major* PPG contains one or several different polypeptide backbones. Protein sequencing of large amounts of purified PPG (>20 μg of amino acids) indicates N-terminal blockage of the polypeptide(s). Immunoblots of HF-treated PPG identify two major protein bands with apparent molecular mass of approximately 70 and >94 kDa, Since dephosphorylation by aqueous HF does not commonly lead to peptide bond cleavage ((45, 58), BSA in this study), these protein bands may correspond to the intact polypeptide backbone(s). However, a large proportion of the protein appears to aggregate on SDS-polyacrylamide gels as well as in the presence of 6 M GdmCl (see Fig. 9*c*) and therefore escapes more detailed analysis. Similar aggregation and insolubility after HF treatment is observed for phosvitin and may be an inherent property of very serine-rich polypeptide stretches, since synthetic polyserine (M_r 10,000) is insoluble in aqueous solutions and does not form defined bands on SDS-PAGE.[2] Thermolysin digestion of *L. major* PPG yields large proteinase-resistant glycopeptides, which are composed almost exclusively of Ser, Ala, and Pro (>97%). Since thermolysin is able to hydrolyze peptide bonds involving Ala (54), it is likely that the protein backbone in these regions of PPG is completely shielded by phosphoglycans against the proteinase.

Mild acid hydrolysis conditions used to deglycosylate PPG led unexpectedly to peptide bond cleavage in BSA, most likely at hypersensitive sites like peptide bonds involving Asp (55). Phosvitin and PPG appear to be degraded to an even larger extent under these conditions, although their Asp content is low ((56) and this study). This result may be explained by a lability of the abundant Ser(P) peptide bonds to mildly acidic conditions, as previously suggested for phosphophoryn (57). Frequent cleavage by mild acid in Ser, Ala, Pro-rich regions and acid precipitation of the peptide fragments depleted of these amino acids may explain the occurrence of a dominant soluble peptide fraction with a composition strikingly similar to the thermolysin-resistant peptides.

A possible structural model for *L. major* PPG based on the results of this study is shown in Fig. 12. The majority of the PPG protein backbone is organized in one or several highly glycosylated and proteinase-resistant regions consisting almost exclusively of Ser, Ala, and Pro, which may be sensitive to mild acid treatment. In these region(s), more than half of the amino acids corresponds to Ser(P) linked to phosphoglycan chains. These consist of a linear array of, on average, three phosphodiester-linked oligosaccharide repeats (a combination of either P2, P3, P4a, or P4b) terminated by a neutral glycan (either N2, N2′, or N3). The structure of the individual glycan chains is unknown. HMBC spectroscopy indicates that the majority of N2 could be linked directly to Ser(P) and not to the PO_4-6-Gal. PPG also appears to contain one or several smaller peptide region(s) accessible to proteinases like thermolysin. These regions exhibit a more diverse amino acid composition including abundant hydrophobic residues (compare Table III, column 5) providing the cleavage sites for the enzyme and may be less extensively glycosylated. The relative arrangement and the number of the different polypeptide regions remains to be determined and will require the cloning of the gene(s) of PPG.

Low mobility and broad bands on SDS-PAGE similar to those observed for the native *L. major* PPG have been described for the highly glycosylated mammalian mucins. Many of the ex-

perimental difficulties encountered in deglycosylation experiments with PPG like peptide bond cleavage, insolubility, and aggregation of the resulting polypeptides and abnormal migration behavior on SDS-polyacrylamide gels have been observed frequently in studies on mammalian mucins ((59–62) and references therein). Many distinct properties of PPG like the very high carbohydrate content (>75% w/w), the large proportion of glycosylated amino acids (>43 mol %) in the protein backbone, the large apparent molecular mass (>2000 kDa), the high negative charge, the filamentous ultrastructure, the formation of networks as well as the high viscosity, and gel formation of concentrated solutions are also reminiscent of this class of glycoproteins (59). In particular, the phosphoglycan-modified and proteinase-resistant Ser(P), Ala, and Pro-rich regions of *L. major* PPG might be analogous to the Thr, Ser, and Pro-rich repeating sequences, which form the extended, rod-like, highly glycosylated and proteinase-resistant polypeptide domains of many mucins (reviewed in Refs. 59–62). PPG may therefore well qualify as a parasite structural equivalent to mammalian mucins.

Ultrastructural studies on sandflies infected with a variety of *Leishmania* species have shown a filamentous, gel-like, carbohydrate-rich matrix in the anterior abdominal and the cardiac regions. The matrix contains large amounts of immobilized procyclic promastigotes and appears to block the cardia and the stomodeal valve of the sandfly (63–69). Interestingly, the infective stage of the parasites, the metacyclic promastigotes, has been reported as being highly motile and unaffected by this gel (69). It has been proposed that this blocking of the digestive tract has a crucial function for the transmission of metacyclic *Leishmania* promastigotes during the second bloodmeal of the sandfly (63, 64, 70–72). Lang and co-workers (73) observed strong labeling of this gel-like filamentous material with anti-LPG mAbs in *L. major*-infected sandflies. The authors assumed these antibodies to be specific for LPG and assigned the labeling to LPG secretion by the parasite and deposition of the glycolipid on the filaments. We have recently proposed that filamentous PPG forms the scaffold of this gelatinous matrix (3, 20). While it is likely that other secreted phosphoglycan antigens like LPG, PG, and sAP ("excreted factor," reviewed in Refs. 1, 3) are also present in the carbohydrate-rich matrix, the filamentous nature and the gel-forming properties of PPG may be crucial for the immobilization of parasites and plug formation at the stomodeal valve. More detailed studies on the function of PPG for the development and survival of procyclic promastigotes in the sandfly and for the transmission of metacyclic promastigotes to the mammalian host will be required to fully assess its role in the parasite life cycle in the insect. Preliminary immunofluorescence and immunoelectron microscopy experiments suggest the presence of PPG-related molecules also in *L. major* amastigotes,[4] which indicates potential functions of the antigen for the mammalian stage of the parasite. The availability of pure PPG, the information about its structure, and the generation of polypeptide-specific antibodies opens the way for the functional analysis and the cloning of the gene(s) of this unusual parasite antigen.

Acknowledgments—We thank Prof. Dr. Peter Overath for support and helpful discussions, Robert Moritz for N-terminal sequencing and amino acid analysis, and Joan Curtis, Dorothee Harbecke, James Eddes, Eva Lau, and Dina Chen for expert technical assistance. We are also grateful to Dr. Gerd Multhaup for performing amino acid analysis and N-terminal sequencing in the initial stages of the study.

REFERENCES

1. Turco, S. J., and Descoteaux, A. (1992) *Annu. Rev. Microbiol.* **46,** 65–94
2. McConville, M. J., and Ferguson, M. A. J. (1993) *Biochem. J.* **294,** 305–324
3. Ilg, T., Stierhof, Y.-D., Wiese, M., McConville, M. J., and Overath, P. (1994) *Parasitology* **108,** S63–S71
4. Orlandi, P. A., Jr., and Turco, S. J. (1987) *J. Biol. Chem.* **262,** 10384–10391
5. Turco, S. J., Hull, S. R., Orlandi, P. A., Jr., Shepherd, S. D., Homans, S. W., Dwek, R. A., and Rademacher, T. W. (1987) *Biochemistry* **26,** 6233–6238
6. Turco, S. J., Orlandi, P. A., Jr., Homans, S. W., Ferguson, M. A. J., Dwek, R. A., and Rademacher, T. W. (1989) *J. Biol. Chem.* **264,** 6711–6715
7. McConville, M. J., Thomas-Oates, J. E., Ferguson, M. A. J., and Homans, S. W. (1990) *J. Biol. Chem.* **265,** 19611–19623
8. McConville, M. J., Schnur, L. F., Jaffe, C., and Schneider, P. (1995) *Biochem. J.* **310,** 807–818
9. Ilg, T., Etges, R., Overath, P., McConville, M. J., Thomas-Oates, J., Thomas, J., Homans, S. W., and Ferguson, M. A. J. (1992) *J. Biol. Chem.* **267,** 6834–6840
10. Thomas, J. R., McConville, M. J., Thomas-Oates, J. E., Homans, S. W., Ferguson, M. A. J., Gorin, P. A. J., Greis, K. D., and Turco, S. J. (1992) *J. Biol. Chem.* **267,** 6829–6833
11. McConville, M. J., Turco, S. J., Ferguson, M. A. J., and Sacks, D. L. (1992) *EMBO J.* **11,** 3593–3600
12. Moody, S. F., Handman, E., McConville, M. J., and Bacic, A. (1993) *J. Biol. Chem.* **268,** 18457–18466
13. Bates, P. A., Hermes, I., and Dwyer, D. M. (1990) *Mol. Biochem. Parasitol.* **39,** 247–255
14. Jaffe, C. L., Perez, L., and Schnur, L. F. (1990) *Mol. Biochem. Parasitol.* **41,** 233–240
15. Ilg, T., Menz, B., Winter, G., Russell, D. G., Etges, R., Schell, D., and Overath, P. (1991) *J. Cell. Sci.* **99,** 175–180
16. Ilg, T., Harbecke, D., Wiese, M., and Overath, P. (1993) *Eur. J. Biochem.* **217,** 603–615
17. Ilg, T., Stierhof, Y.-D., Etges, R., Adrian, M., Harbecke, D., and Overath, P. (1991) *Proc. Natl. Acad. Sci. U. S. A.* **88,** 8774–8778
18. Ilg, T., Overath, P., Ferguson, M. A. J., Rutherford, T., Campbell, D. G., and McConville, M. J. (1994) *J. Biol. Chem.* **269,** 24073–24081
19. Wiese, M., Ilg, T., Lottspeich, F., and Overath, P. (1995) *EMBO J.* **14,** 1067–1074
20. Stierhof, Y.-D., Ilg, T., Russell, D. G., Hohenberg, H., and Overath, P. (1994) *J. Cell. Biol.* **125,** 321–331
21. Brun, R., and Schonenberger, M. (1979) *Acta Trop.* **36,** 289–292
22. Peterson, G. L. (1983) *Methods Enzymol.* **91,** 95–119
23. Bartlett, G. R. (1959) *J. Biol. Chem.* **234,** 466–468
24. Kelleher, M., Bacic, A., and Handman, E. (1992) *Proc. Natl. Acad. Sci. U. S. A.* **89,** 6–10
25. Laemmli, U. K. (1970) *Nature* **227,** 680–685
26. Towbin, H., Staehelin, T., and Gordon, J. (1979) *Proc. Natl. Acad. Sci. U. S. A.* **76,** 4350–4354
27. Heukeshoven, J., and Dernick, R. (1988) *Electrophoresis* **9,** 28–32
28. Turco, S. J., Wilkerson, M. A., and Clawson, D. R. (1984) *J. Biol. Chem.* **259,** 3883–3889
29. Lau, E., and Bacic, A. (1993) *J. Chromatogr.* **637,** 100–103
30. Ferguson, M. A. J., Homans, S. W., Dwek, R. A., and Rademacher, T. W. (1988) *Science* **239,** 753–759
31. Fox, A., Morgan, S. L., and Gilbert, J. (1989) in *Analysis of Carbohydrates by GLC and MS* (Biermann, C. J., and McGinnis, G., eds) CRC Press, Inc., Boca Raton, FL
32. Oxley, D., and Bacic, A. (1995) *Glycobiology* **5,** 517–523
33. Tyler, J. M., Anderson, J. M., and Branton, D. (1980) *J. Cell Biol.* **85,** 489–495
34. Handman, E., Greenblatt, C. L., and Goding, J. W. (1984) *EMBO J.* **3,** 2301–2306
35. Greis, K. D., Turco, S. J., Thomas, J. R., McConville, M. J., Homans, S. W., and Ferguson, M. A. J. (1992) *J. Biol. Chem.* **267,** 5876–5881
36. Rickwood, D., and Chambers, J. A. A. (1984) in *Centrifugation* (Rickwood, D., ed) 2nd Ed., pp. 95–125, IRL Press at Oxford University Press, Oxford
37. Ilg, T. (1992) *Sekretierte Antigene von Leishmania Promastigoten: Strukturelle und biochemische Charakterisierung von Lipophosphoglycan und sekretierter saurer Phosphatase.* Ph.D thesis, Eberhard-Karls-Universität Tübingen, FRG
38. Harlow, E., and Lane, D. (1988) *Antibodies: A Laboratory Manual,* Cold Spring Harbor Laboratory, Cold Spring Harbor, NY
39. Helander, A., Kenne, L., Oscarson, S., Peters, T., and Brisson, J. R. (1992) *Carbohydr. Res.* **230,** 299–318
40. Ho, C., Magnuson, J. A., Wilson, J. B., Magnuson, N. S., and Kurland, R. J. (1969) *Biochemistry* **8,** 2074–2082
41. Bax, A., Summers, M. F., Egan, W., Guirgis, N., Schneerson, R., Robbins, J. B., Orskov, F., Orskov, I., and Vann, W. F. (1988) *Carbohydr. Res.* **173,** 53–64
42. Leloir, L. F., and Cardini, C. E. (1957) *Methods Enzymol.* **3,** 840–850
43. Taborsky, G. (1974) *Adv. Protein Chem.* **28,** 1–210
44. Shaw, N., and Stead, A. (1974) *Biochem. J.* **143,** 461–464
45. Gustafson, G. L., and Gander, J. E. (1984) *Methods Enzymol.* **107,** 172–183
46. Lovelace, J. K., and Gottlieb, M. (1986) *Am. J. Trop. Med. Hyg.* **35,** 1121–1128
47. McConville, M. J., and Bacic, A. (1990) *Mol. Biochem. Parasitol.* **38,** 57–68
48. McConville, M. J., and Homans, S. W. (1992) *J. Biol. Chem.* **267,** 5855–5861
49. Carver, M. A., and Turco, S. J. (1991) *J. Biol. Chem.* **266,** 10974–10981
50. Carver, M. A., and Turco, S. J. (1992) *Arch. Biochem. Biophys.* **295,** 309–317
51. Ng, K. F., Handman, E., and Bacic, A. (1994) *Glycobiology* **4,** 845–853
52. Stetler-Stevenson, W. G., and Veis, A. (1983) *Biochemistry* **22,** 4326–4335
53. Ilg, T., Stierhof, Y.-D., McConville, M. J., and Overath, P. (1995) *Eur. J. Cell Biol.* **66,** 205–215
54. Boehringer Mannheim (1987) *Boehringer Mannheim Biochemica Information,* Mannheim, FRG
55. Inglis, A. S. (1983) *Methods Enzymol.* **91,** 324–332
56. Byrne, B. M., van het Schip, A. D., van de Klundert, J. A. M., Arnberg, A. C., Gruber, M., and AB, G. (1984) *Biochemistry* **23,** 4275–4279
57. Sabsay, B., Stetler-Stevenson, W. G., Lechner, J. H., and Veis, A. (1991)

[4] E. Handman and T. Ilg, unpublished experiments.

Biochem. J. **276,** 699–707
58. Prescott, D. J., Elovson, J., and Vagelos, P. R. (1969) *J. Biol. Chem.* **244,** 4517–4521
59. Strous, G. J., and Dekker, J. (1992) *Crit. Rev. Biochem. Mol. Biol.* **27,** 57–92
60. Corfield, T. (1992) *Glycoconj. J.* **9,** 217–221
61. Rose, M. C. (1992) *Am. J. Physiol.* **7,** L413–L429
62. Verma, M., and Davidson, E. A. (1994) *Glycoconj. J.* **11,** 172–179
63. Killick-Kendrick, R. (1979) in *Biology of the Kinetoplastida* (Lumsden, W. H. R., and Evans, D. A., eds) Vol. 2, 395–460, Academic Press, New York
64. Killick-Kendrick, R., Wallbanks, K. R., Molyneux, D. H., and Lavin, D. R. (1988) *Parasitol. Res.* **74,** 586–590
65. Walters, L. L., Modi, G. B., Tesh, R. B., and Burrage, T. (1987) *Am. J. Trop. Med. Hyg.* **36,** 294–314
66. Walters, L. L., Modi, G. B., Chaplin, G. L., and Tesh, R. B. (1989) *Am. J. Trop. Med. Hyg.* **41,** 295–317
67. Walters, L. L., Chaplin, G. L., Modi, G. B., and Tesh, R. B. (1989) *Am. J. Trop. Med. Hyg.* **40,** 19–39
68. Lawyer, P. G., Young, D. G., Butler, J. F., and Akin, D. E. (1987) *J. Med. Entomol.* **24,** 347–355
69. Lawyer, P. G., Ngumbi, P. M., Anjili, C. O., Odongo, S. O., Mebrahtu, Y. B., Githure, J. I., Koech, D. K., and Roberts, C. R. (1990) *Am. J. Trop. Med. Hyg.* **43,** 31–43
70. Warburg, A., and Schlein, Y. (1986) *Am. J. Trop. Med. Hyg.* **35,** 926–930
71. Beach, R., Kiilu, G., and Leeuwenburg, J. (1985) *Am. J. Trop. Med. Hyg.* **34,** 278–282
72. Jefferies, D., Livesey, J. L., and Molyneux, D. H. (1986) *Acta Trop.* **43,** 43–53
73. Lang, T., Warburg, A., Sacks, D. L., Croft, S. L., Lane, R. P., and Blackwell, J. M. (1991) *Eur. J. Cell Biol.* **55,** 362–372